Unusual Non-neoplastic Pulmonary Conditions

8

Annikka Weissferdt

In this chapter, various unusual non-neoplastic pulmonary disorders are discussed. This group of lesions encompasses a range of different conditions that may be of multifactorial, immunologic, genetic, or uncertain etiology. Awareness of the existence of these relatively rare disorders and their histopathological characteristics is necessary for the pathologist in order to avoid misdiagnosis. In this context, the conditions reviewed include *pulmonary placental transmogrification, pulmonary alveolar proteinosis, pulmonary alveolar microlithiasis, diffuse pulmonary ossification, pulmonary calcification, pulmonary hyalinizing granuloma, pulmonary amyloidosis*, and *pulmonary light chain deposition disease*.

8.1 Pulmonary Placental Transmogrification

Pulmonary placental transmogrification (PPT) is a rare benign condition of the lung that was first described in abstract form by McChesney in 1979 as an unusual cystic lesion [1]. The term *placental transmogrification* was chosen to describe a process whereby the pulmonary parenchyma undergoes severe emphysematous change with formation of fibrous papillary structures closely resembling the chorionic villi of the placenta [1]. The pathogenesis of this condition is largely unknown, and several different hypotheses have been put forward to account for this phenomenon, but most authors appear to agree that PPT represents a variant of bullous emphysema [2–4]. Histologically, a range of features can be seen in these lesions which have led to a variety of designations for this condition, including *placentoid bullous lesion of the lung* [5] and *pulmonary lipomatosis* [6]. Ultimately, all theses conditions seem to represent lesions in the spectrum of PPT [7].

8.1.1 Clinical Features

PPT has been reported in patients with an age range from 24 to 72 years and with an average age at diagnosis of 46 years. About half of the patients have a history of smoking, and the majority of patients are men [5, 8, 9]. Presenting symptoms primarily include chest pain, cough, chronic obstructive lung disease, and pneumothorax. Concurrent emphysematous changes and the presence of pulmonary chondroid hamartomas are other common associations [8]. Radiologically, the lesions are typically unilateral intrapulmonary bullous cysts or more rarely solid lung masses [7, 8, 10]. PPT is an entirely benign lesion that is curable with lung-sparing surgical resection leading to rapid improvement of symptoms and quality of life. To date, no recurrences have been reported after surgical treatment [10].

8.1.2 Pathological Features

Gross examination of lungs with PPT reveals the presence of cystic lesions filled with vesicular, grape-like, or spongy material, closely resembling molar placental tissue [11, 12]. Microscopically, the lung parenchyma is collapsed and replaced by numerous papillary structures with progression of changes ranging from stromal cores composed of oval- or spindle-shaped cells and proliferation of vascular channels to cores primarily filled by adipose and/or lymphoid tissue with germinal centers (Fig. 8.1a–d). Further changes include edematous stromal cores with single vascular channels or sclerosis of the papillary structures (Fig. 8.2a, b). The papillary structures are typically lined by an epithelium that is flat, cuboidal, or columnar and can be ciliated (Fig. 8.3). The border to the surrounding uninvolved lung is usually non-descript, and the lesions often merge with emphysematous lung parenchyma [2, 7].

8.1.3 Immunohistochemical Features

The immunohistochemical phenotype of PPT is incompletely described; however, from the published data, it appears that the epithelial cells lining the papillary structures

A. Weissferdt, *Diagnostic Thoracic Pathology*, https://doi.org/10.1007/978-3-030-36438-0_8

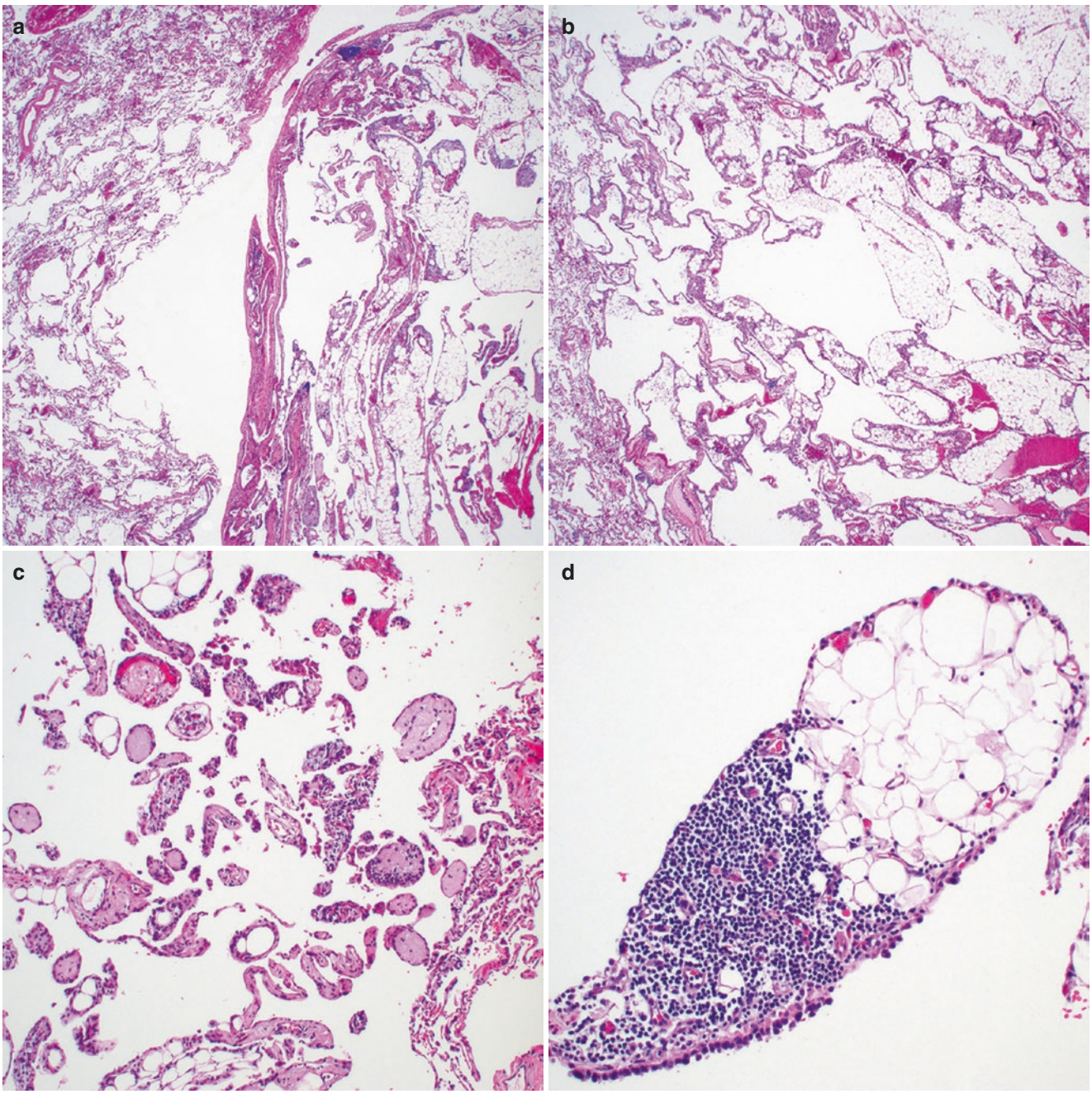

Fig. 8.1 (**a**) Low power view of a lung with placental transmogrification showing replacement of the lung parenchyma by numerous papillary structures; (**b**) the air spaces are distorted resulting in an emphysematous appearance; (**c**) the papillary structures often closely resemble the chorionic villi of the placenta; (**d**) the papillary cores can be composed of adipose or lymphoid tissue

are immunoreactive for pancytokeratin and TTF-1, while the stromal cells within the cores are positive for CD10 and vimentin [8, 13, 14].

8.1.4 Differential Diagnosis

Based on the varied histopathological presentation of PPT, the differential diagnosis includes vascular lesions such as hemangioma or lymphangioma, pneumocytoma (sclerosing hemangioma), or bullous emphysema. Compared to PPT, pulmonary hemangiomas or lymphangiomas are more infiltrative lesions involving the lung parenchyma containing spaces filled with blood or lymph. Pneumocytomas are well-circumscribed benign tumors of the lung that typically affect middle-aged to older female patients. Microscopically, pneumocytomas are characterized by the simultaneous presence of papillary, angiomatoid, solid, and sclerotic patterns as

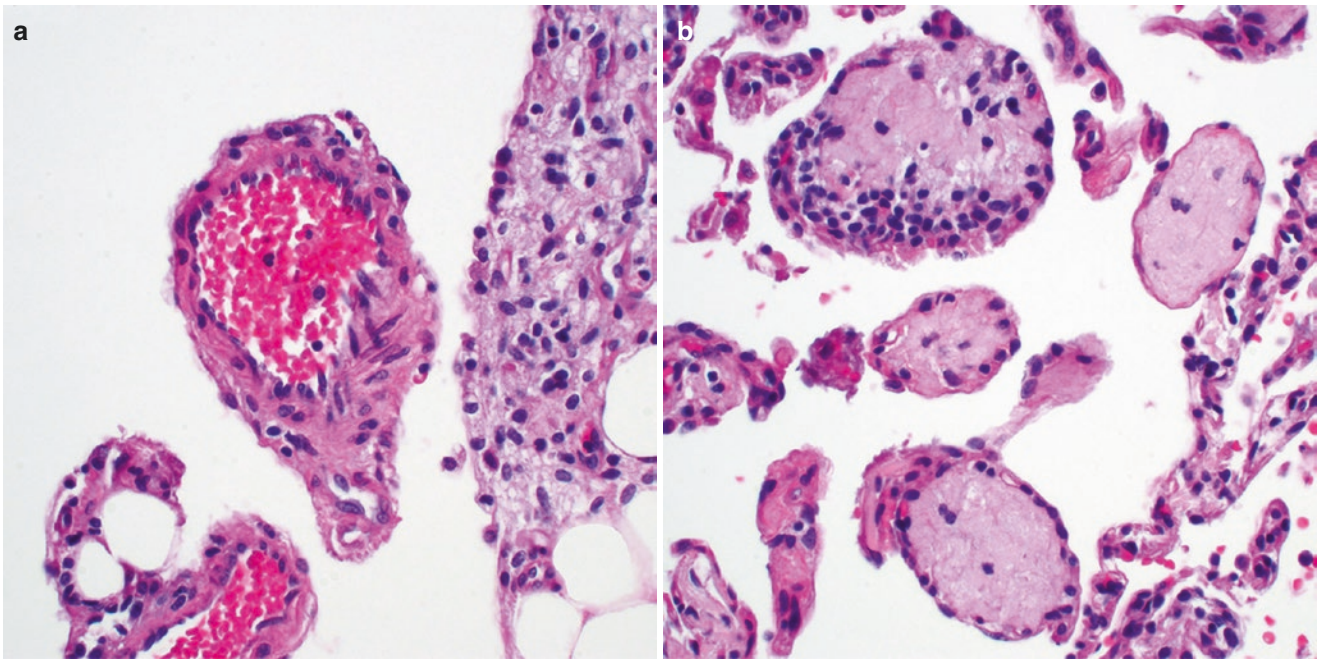

Fig. 8.2 (**a**) Some of the papillary cores in placental transmogrification of the lung can contain prominent vascular channels; (**b**) other papillae show dense sclerotic changes

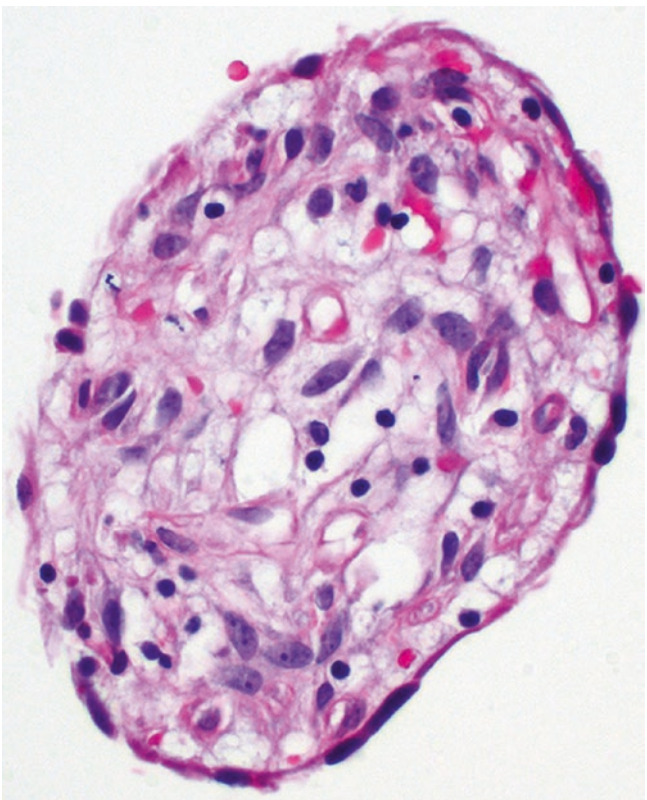

Fig. 8.3 The epithelial lining of the papillary structures in placental transmogrification is typically flat or cuboidal in nature but can also be composed of columnar or ciliated epithelium

well as a dual tumor cell population comprising epithelial lining cells and stromal round cells. This simultaneous presence of multiple growth patterns and dual cell population are not features typically associated with PPT. Furthermore, the unilateral cystic appearance of PPT can be distinguished from the bilateral diffuse involvement of the lung in bullous emphysema which typically affects an older smoker population.

8.2 Alveolar Proteinosis

Pulmonary alveolar proteinosis (PAP) is a rare disorder that leads to the accumulation of lipoproteinaceous surfactant components in the alveolar spaces. The disease was first described by Rosen in 1958 describing 27 patients with this remarkable condition [15]. Since its first description, PAP has been recognized to occur in three clinically distinct forms: *congenital, primary (idiopathic or autoimmune)*, and *secondary* although the vast majority of cases occur in adults in the autoimmune setting (>90%) [16]. Irrespective of clinical subtype, the resultant disturbance will lead to physical manifestations ranging from asymptomatic disease to full-blown respiratory failure [17]. Recent advances in this disease have led to the discovery of some of the mechanisms underlying the pathogenesis of PAP which seems to vary in the three different types. *Congenital PAP* is attributed to a genetic defect due to

mutations affecting the *surfactant protein B (SFTPB), ABC transporter 3 (ABCA3)*, or *colony-stimulating factor 2 receptor beta (CSF2RB) genes*. Mutations in these genes can lead to failure of production of mature surfactant B, reduced or absent expression of the protein, or functional deficiency of granulocyte-monocyte colony-stimulating factor (GM-CSF) [16]. Deficiency of GM-CSF due to neutralizing autoantibodies is responsible for the development of *idiopathic or autoimmune PAP*. Involvement of GM-CSF in human cases of PAP was suspected after the discovery that knockout mice deficient in GM-CSF developed lung lesions similar to PAP [18, 19]. *Secondary PAP* has been associated with environmental exposure to toxins or dusts and hematological disorders for which defective alveolar macrophage function or reduction in their number due to cytopenia is the likely causative mechanism [20, 21]. Regardless of the underlying etiology, all forms of PAP will lead to the accumulation of phospholipid material and cellular debris within alveolar spaces diminishing gas exchange and resulting in respiratory distress and potentially death [22].

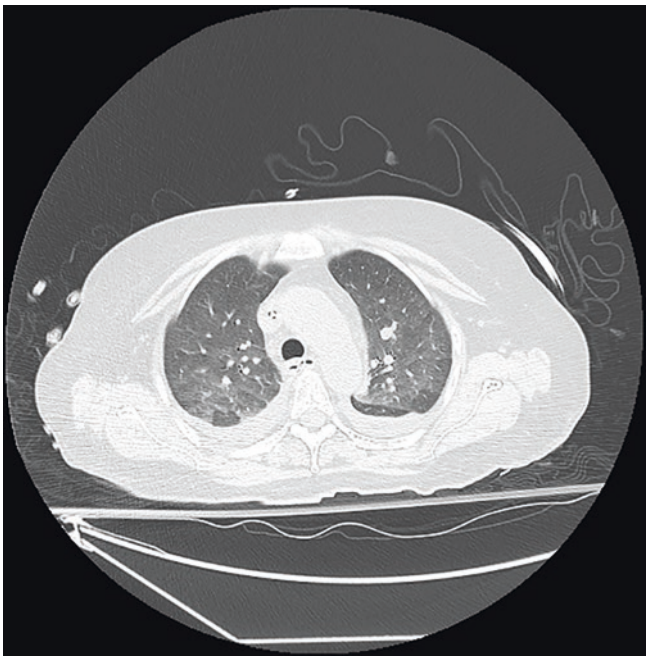

Fig. 8.4 Computed tomography scan of the chest of a patient with pulmonary alveolar proteinosis shows patchy ground glass opacities in both lungs resulting in a "crazy paving" pattern; bilateral pleural effusions can also be noted

8.2.1 Clinical Features

Clinical history, including family history of pulmonary disease, consanguinity, history of hematologic disorder, and age at onset are important parameters in the workup of patients with suspected PAP. While congenital PAP usually presents immediately after birth or after a postnatal, symptom-free period ranging from a few weeks to several years, patients with autoimmune and secondary PAP are almost always adults with a peak age at diagnosis in the 3rd to 6th decade and near equal sex ratio. The main symptoms are often nonspecific and in the congenital form include progressive onset of dyspnea during feeding or exercise and later at rest as well as cough, cyanosis, and digital clubbing. Clinical disease in adult patients is usually characterized by an insidious onset of dyspnea, cough, weight loss, hemoptysis, fever, and production of milky white frothy sputum. A more acute presentation may occur in a minority of patients with rapid progression to respiratory failure and death. On the other hand, up to 30% of patients are asymptomatic at presentation, and the disease is diagnosed during workup for unrelated reasons [16, 23]. Chest radiographs of patients with PAP typically show bilateral symmetric ill-defined nodular or confluent alveolar filling patterns with a perihilar or basal distribution. Rare cases may also show asymmetric, unilateral, peripheral, or lobar patterns [24]. High-resolution CT shows smooth interlobar or intralobar septal thickening superimposed on a background of ground glass opacities producing a characteristic *crazy paving* pattern [25] (Fig. 8.4). Although this pattern is not entirely pathognomonic for PAP, the combination of typical clinical features, such as slow onset of the disease coupled with the characteristic radiological features as well as the dissociation between clinical and radiological findings, facilitates its diagnosis. The treatment and prognosis of PAP largely depends on the underlying etiology. Mild forms of the congenital disease can be treated with supportive therapy only, while whole-lung lavage and lung transplantation may be required in more severe cases [26]. Optimal management for patients with the secondary form of PAP requires therapy directed against the causative disorder along with supportive respiratory care [27]. Whole-lung lavage remains the gold standard of therapy for patients with idiopathic PAP. Supplemental GM-CSF therapy, plasmapheresis to reduce GM-CSF antibodies, and rituximab are additional therapeutic options [28–30]. The survival for patients with idiopathic PAP lies in the order of 85–94% at 5 years [31], while reports on patients with congenital PAP indicate a poor prognosis with survival measured in days or months [32, 33].

8.2.2 Pathological Features

The histological features of all types of PAP are similar irrespective of the underlying etiology. The characteristic feature is the filing of alveolar spaces with an amorphous granular or globular periodic acid Schiff (PAS)-positive eosinophilic material intermixed with cellular debris derived

from degenerating alveolar macrophages, detached pneumocytes, and cholesterol clefts (Fig. 8.5a–c). The alveolar architecture is typically preserved, but alveolar walls may thicken over time and progress to pulmonary fibrosis (Fig. 8.6). Typically, a slight retraction space separates the alveolar walls from the exudate (Fig. 8.7). Type II pneumocyte hyperplasia may be seen lining these walls, and the surrounding alveoli may show emphysematous changes or lymphocytic infiltration [16, 23].

8.2.3 Laboratory Diagnosis, Histochemical Stains, and Immunohistochemical Stains

Apart from physical examination, clinical history, and radiologic imaging, bronchoalveolar lavage (BAL) fluid can be helpful in the diagnosis of PAP. Characteristically, BAL fluid from patients with PAP is milky and opaque and settles into a thick sediment layer and a translucent supernatant.

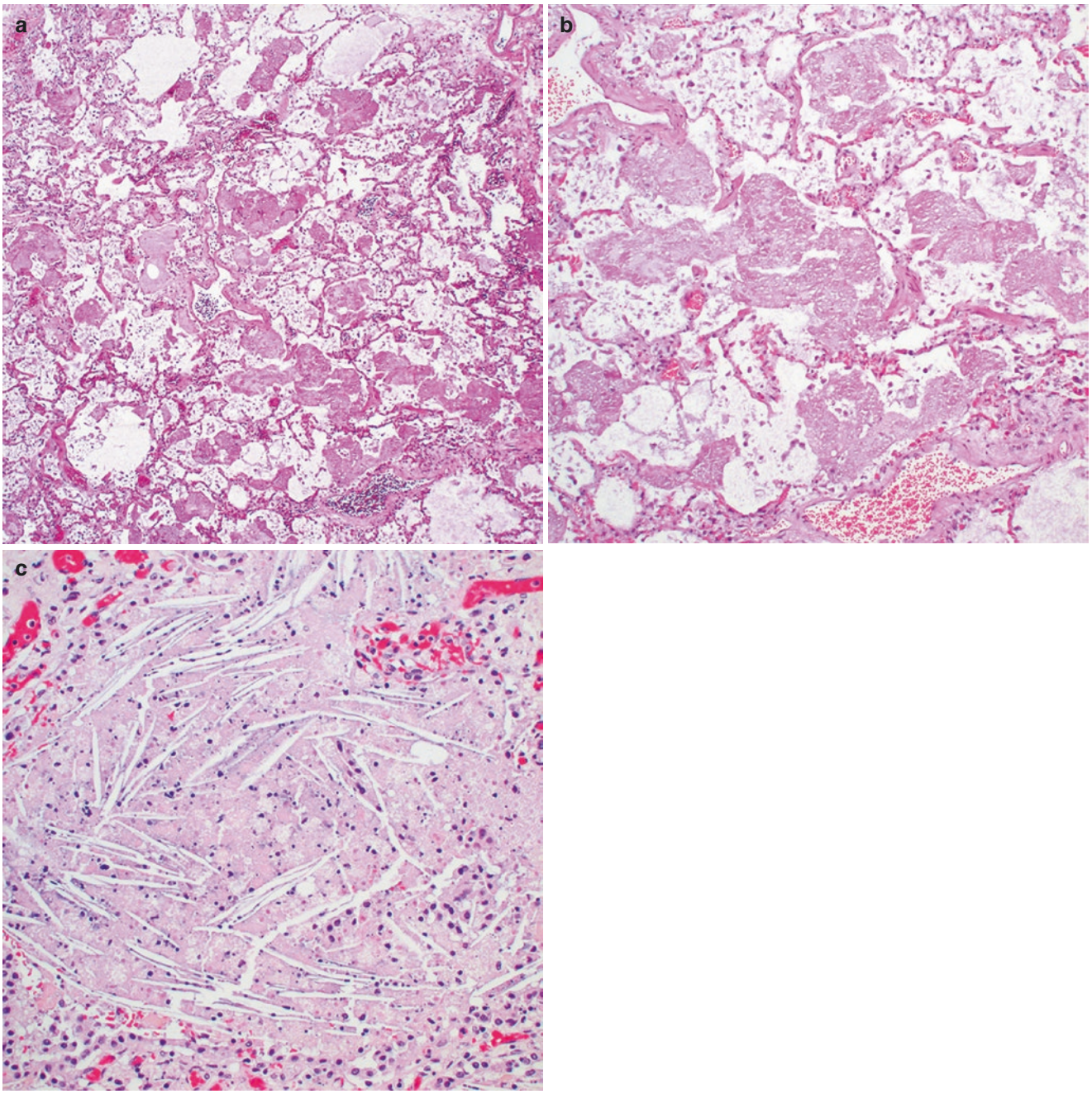

Fig. 8.5 (**a**) Low power view of a case of pulmonary alveolar proteinosis demonstrates alveolar spaces filled with deeply eosinophilic material; (**b**) this material is typically amorphous and has a granular appearance; (**c**) cellular debris and cholesterol clefts within the proteinaceous exudate are other typical findings in this condition

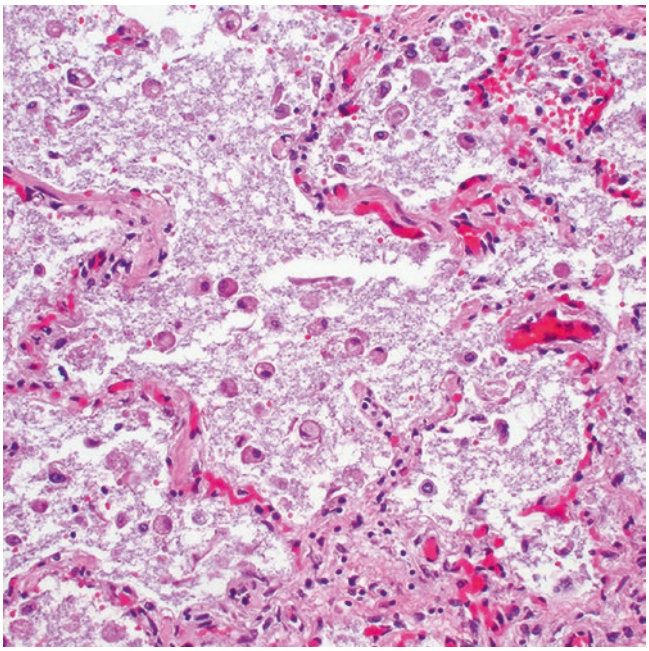

Fig. 8.6 Mild thickening of alveolar septa may be seen in pulmonary alveolar proteinosis and may over time progress to interstitial fibrosis

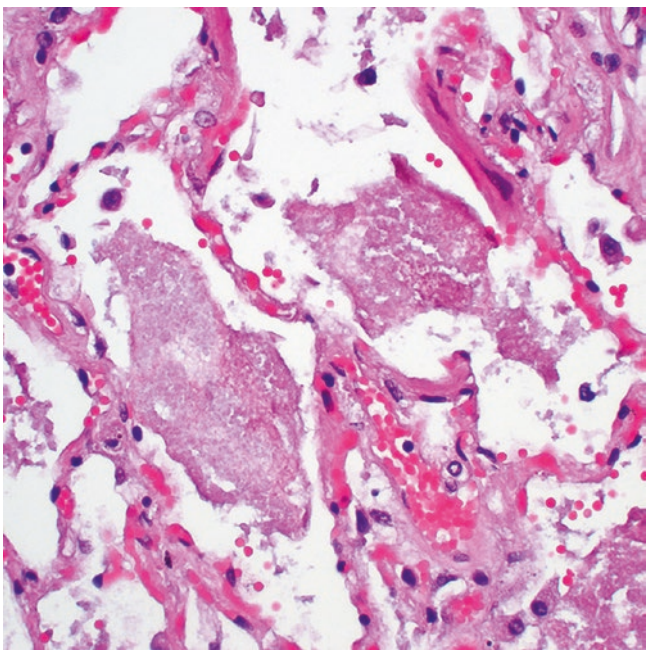

Fig. 8.7 The exudate in pulmonary alveolar proteinosis is often separated from the alveolar walls by a small area of retraction

Enlarged foamy alveolar macrophages engorged with diastase-resistant PAS-positive intracellular inclusions are a striking feature [34, 35]. BAL fluid and electron microscopy analysis of tissue sections will also reveal concentrically laminated bodies called *lamellar bodies* that are considered diagnostic of PAP [36, 37]. Lung biopsy is currently considered the gold standard for diagnosis of the disease and can be supported by molecular techniques and genetic testing in cases of congenital PAP and detection of GM-CSF antibodies by latex agglutination test for idiopathic PAP. Immunohistochemically, the granular material is reactive with antibodies directed against surfactant protein; histochemical studies will reveal that the granular material is diffusely positive for PAS (Fig. 8.8a, b).

8.2.4 Differential Diagnosis

Intraalveolar accumulation of proteinaceous material may also be observed in other pathologic conditions and in this context, the differential diagnosis for PAP primarily includes pulmonary edema and pneumocystis pneumonia. The latter typically has a more dramatic clinical presentation, a more foamy-appearing finely vacuolated exudate, and a higher degree of inflammatory changes in the background lung parenchyma. Pulmonary edema on the other hand lacks the granular material and cellular debris that are characteristically associated with PAP.

8.3 Alveolar Microlithiasis

Pulmonary alveolar microlithiasis (PAM) is a rare autosomal-recessive genetic lung disorder that is characterized by numerous calcifications filling the alveolar spaces. First recognized as a distinct disease by Harbitz in 1918 [38], it was not until 1933 that Ludwig Puhr named the process *"Mikrolithiasis alveolaris pulmonum"* [39]. The underlying cause for this condition remained unknown for a long time until it emerged that homozygous mutations in the gene *solute carrier family 34 (sodium phosphate), member 2 (SLC34A2)* are significantly related to the development of PAM [40]. This gene encodes a membrane protein (type IIb sodium-dependent phosphate transporter) that is primarily expressed in the apical portions of alveolar type II cells and is the most common phosphate carrier in the lungs [41]. Mutations affecting *SLC34A2* can thereby lead to loss of gene expression, the production of a defective protein or result in the formation of concretions or microliths composed of calcium and phosphorus in the alveolar spaces [42, 43]. The occurrence can be sporadic or familial with up to 1/3 of cases being hereditary [44]. The disease has a long and protracted clinical course with gradual loss of lung function, respiratory failure, pulmonary hypertension, and eventually cor pulmonale and death. No particular geographic distribution has been identified, although the disease seems to be most prevalent in Turkey, Italy, and the United States [45].

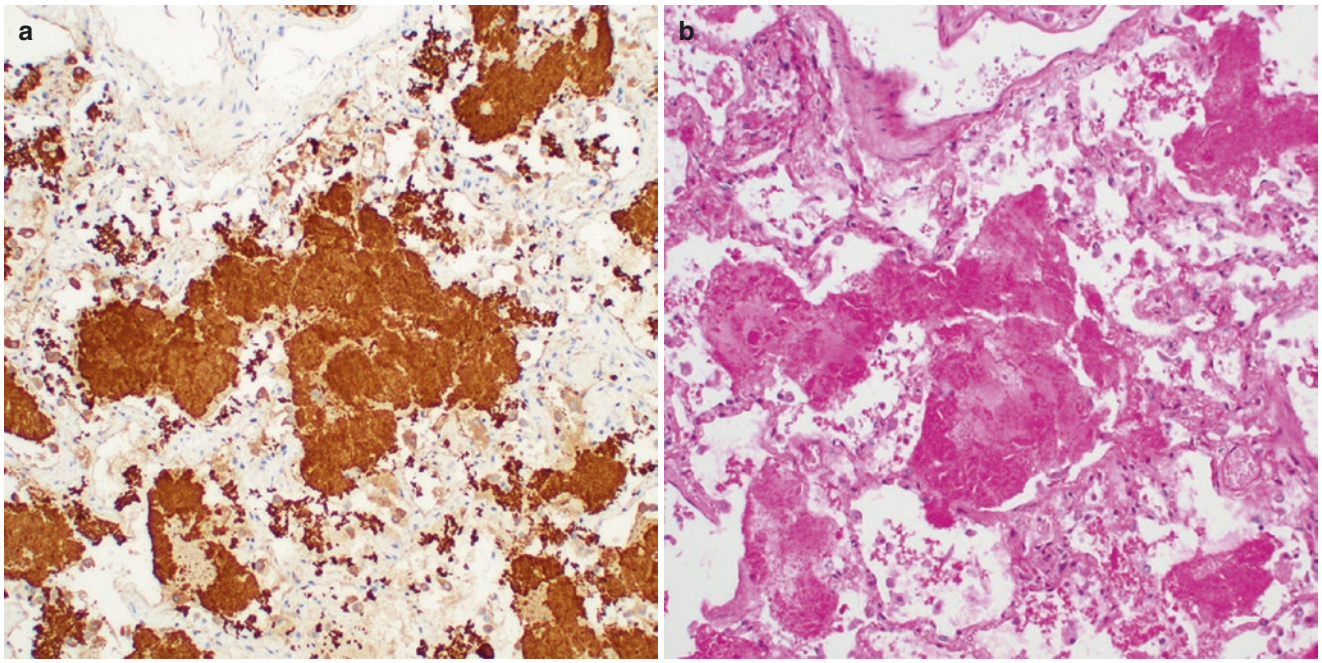

Fig. 8.8 (**a**) Strong reactivity of the exudate in pulmonary alveolar proteinosis with surfactant protein by immunohistochemistry; (**b**) the material is also brightly positive with a periodic acid-Schiff (PAS) histochemical stain

8.3.1 Clinical Features

PAM can affect individuals at any age but patients normally become symptomatic in the 3rd to 4th decade of life. Males and females are equally affected with no specific gender predilection. The hallmark of PAM is the dissociation between the paucity of clinical findings compared to the imaging findings. Often the patients are entirely asymptomatic and their disease is only detected incidentally, while others present with symptoms such as chest pain, dyspnea, dry cough, gradual decrease in exercise tolerance, or sporadic hemoptysis [42]. Pulmonary function tests initially remain normal but as the disease progresses will show a restrictive pattern [46]. PAM usually progresses within 10–20 years from the time of diagnosis; however, reported follow-up periods can be as long as more than 40 years [45, 47]. Death typically occurs 10–15 years after diagnosis usually as a result of respiratory failure secondary to pulmonary hypertension and cor pulmonale [41]. Extrapulmonary manifestations associated with *SLC34A2* mutations do exist and may vary according to the mutational penetrance. These include medullary nephrocalcinosis, nephrolithiasis, cholelithiasis, calcification of the lumbar spine, testicular involvement, and cardiac valve calcifications [48, 49]. In addition, PAM has been described in association with comorbidities such as pectus excavatum, hypertrophic pulmonary osteoarthropathy, milk-alkali syndrome, diaphyseal aclasia, autosomal-recessive Waardenburg anophthalmia syndrome, and lymphocytic interstitial pneumonitis [50]. Chest X-rays of patients with PAM typically demonstrate diffuse bilateral areas of micronodular calcification, producing a characteristic "sandstorm" appearance. These changes are first apparent in the lower portions, then in the middle portions, and finally in the superior portions of the lung. Other findings include small apical bullae and a black pleural line representing an area of linear hyperlucency caused by small thin-walled subpleural cysts [51, 52]. High-resolution CT shows diffuse ground glass attenuation representing small calcifications in the air spaces in patients with early-stage disease [53]. Subpleural linear calcifications are often apparent and are a reflection of the accumulation of calcifications in the lung periphery mimicking pseudopleural calcifications [53]. Small parenchymal nodules diffusely spread throughout the lung parenchyma as seen on CT correspond to the "sandstorm" picture on plain chest radiographs, while subpleural cysts with diameters of 5–10 mm correlate with the "black pleura sign" on chest X-rays. Areas of ground glass opacity with thickening of the interposed interlobular septa, the so-called crazy paving pattern, are considered highly specific if not pathognomonic of PAM [53, 54]. In fact, the imaging features of PAM are so characteristic that additional diagnostic investigations are often unnecessary, especially in patients with a family history of the disorder [45]. Currently, no effective treatment has been recognized for patients with PAM. The disease may progress to interstitial fibrosis causing pulmonary hypertension, cor pulmonale, and ultimately pulmonary and right heart failure. Systemic steroid treatment and repeated bronchoalveolar lavage have proven ineffective [41], and disodium etidro-

nate, a diphosphonate, has been used in the treatment of PAM with mixed results [50]. Lung transplantation is currently the only effective therapy but should be performed before the disease progresses to an advanced stage [55].

8.3.2 Pathological Features

Gross examinations of the lungs of patients with PAM will show large, heavy, and firm lungs that completely fill the thoracic cavity. The outer surface of the lungs has a granular appearance due to protrusion of microliths into the visceral pleura. The tissue is difficult to cut and will reveal numerous sand-like concretions and dilated spaces containing microliths [42]. Microscopically, the characteristic calcospherites located within dilated alveolar spaces are apparent. These measure 250–750 μm in diameter and consist of concentrically laminated bodies with an onion-skin appearance and amorphous- or granular-appearing nuclei. These microliths lie freely within the alveoli. Complete obliteration of the alveolar spaces can occur with gradual growth and can lead to compression of the alveolar walls and resulting fibrous replacement [39, 42].

8.3.3 Laboratory Diagnosis and Histochemical Stains

The diagnosis of PAM can often be established by the clinical history and typical radiological pattern alone without the need for more invasive procedures [44, 53]. However, in some cases, sputum, bronchoalveolar lavage examination and lung biopsy are performed and will typically reveal the characteristic purple-brown concentric calcifications which may show PAS-positive tinctorial properties [56]. Chemical analysis of these normally yields a phosphorus/calcium ratio of 1:2 consistent with calcium phosphate [42, 57]. Routine blood tests, including serum calcium, and hepatic, renal, and parathyroid function tests are usually within normal limits. Increased serum levels of surfactant A and D have more recently been described in patients with PAM and may be used to monitor disease activity and progression [58].

8.3.4 Differential Diagnosis

The differential diagnosis of PAM includes metastatic or dystrophic pulmonary calcification, pulmonary corpora amylacea, and so-called pulmonary blue bodies. In metastatic or dystrophic calcification, the deposits have a different shape and are typically located in the interstitium, whereas in PAM, deposits are round lamellar calcifications within alveolar spaces. Corpora amylacea are laminated round bodies often found in emphysematous lungs or in the lungs of elderly patients. They demonstrate eosinophilic properties on H&E sections and also differ from microliths by their smaller size (30–200 μm). In addition, calcification is not a feature of pulmonary corpora amylacea. Pulmonary blue bodies are intraalveolar laminated basophilic concretions consisting of calcium carbonate in a mucopolysaccharide matrix. These can be distinguished from pulmonary microliths based on their small size (15–40 μm), different chemical composition, and absence of typical imaging findings for patients with PAM [42].

8.4 Diffuse Pulmonary Ossification

Diffuse pulmonary ossification is an uncommon condition characterized by progressive metaplastic bone formation in the lung parenchyma. Luschka first described diffuse pulmonary ossification in 1856 [59], and more recently two types of the disease have been recognized: dendriform pulmonary ossification (DPO) and nodular pulmonary

Table 8.1 Pertinent characteristics of diffuse pulmonary ossification

	Dendriform pulmonary ossification	Nodular pulmonary ossification
Clinical association	Chronic obstructive lung disease Interstitial pulmonary fibrosis Adult respiratory distress syndrome Organizing pneumonia Pneumoconioses Asbestosis Heavy metal exposure	Chronic cardiac failure Cardiac valve disorders Hypertrophic subaortic stenosis
Radiology	Branching coral-like densities, lower lobe predominant	Multiple calcified nodules, lower lobe predominant
Pathology	Angulated and branching osseous structures with marrow elements and/or fat	Nodules of mature lamellar bone within alveoli, no marrow elements/fat
Treatment and prognosis	Based on treatment of underlying disease; symptomatic relief; slowly progressive	Based on treatment of underlying disease; symptomatic relief; slowly progressive

ossification (NPO) (Table 8.1). The bone formation in either form is thought to represent a metaplastic response to chronic lung injury. What distinguishes the two is the clinical context, the quality, and the location of the bony deposits in the lung. While the ossification in DPO is commonly associated with chronic obstructive pulmonary disease or interstitial pulmonary fibrosis, NPO is often the result of a passive congestive disorder, such as cardiac valve disease or heart failure. Furthermore, histologically, DPO has a dendritic or coral-like appearance growing along the alveolar septa, whereas NPO consists of ossified nodules within the alveolar spaces [60–63] (Table 8.1). Diffuse pulmonary ossification is usually not diagnosed clinically and often only recognized on radiologic imaging or at autopsy. Occasionally, however, pathologic evaluation of surgical specimens becomes necessary requiring awareness of this rare entity in order to correctly identify its features.

8.4.1 Clinical Features

The nodular form of diffuse pulmonary ossification characteristically occurs in a setting of mitral valve stenosis, but it can generally develop with any process leading to chronic pulmonary edema and pulmonary venous hypertension [64]. DPO, on the other hand, is most often seen in patients with pulmonary interstitial fibrosis, especially usual interstitial pneumonitis (UIP), and preferentially affects men in the 5th and 6th decades of life [61, 65–67]. Clinical manifestations in diffuse pulmonary ossification are unusual, and patients are typically asymptomatic or present with minimal complaints, such as cough, dyspnea, or other symptoms related to any underlying lung or cardiac disease [68]. In some cases, pulmonary function tests can show a restrictive pattern and decreased diffusion capacity [68]. Radiologically, DPO often manifests as fine linear branching opacities that may be mistaken for bronchiectasis or interstitial lung disease [62], while NPO shows multiple calcified nodules usually measuring 1–5 mm in diameter, indistinguishable from other types of diffuse parenchymal calcification [69, 70]. Both forms of the disease typically affect the lower lobes of the lung [65]. The clinical course of diffuse pulmonary ossification is indolent with slow progression or stable disease over time but generally depends on the underlying physical condition of the patient. Disease regression has not been described [71, 72]. There is no definitive treatment for the disease other than symptomatic relief although the role of bisphosphonates and warfarin in delaying or preventing ossification of the pulmonary parenchyma is currently undergoing investigation [72].

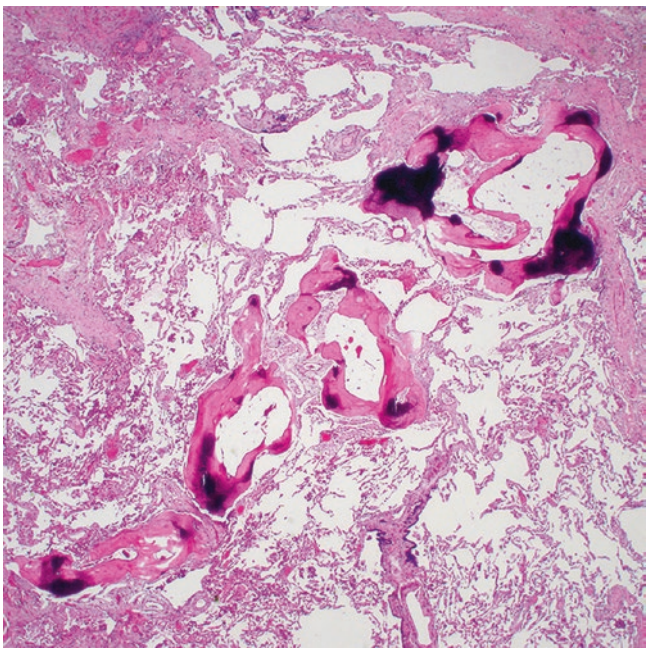

Fig. 8.9 Dendriform pulmonary ossification characterized by bony spicules in the interstitial spaces

8.4.2 Pathological Features

Gross examination of the lungs affected by diffuse pulmonary ossification will show multiple firm to hard nodules or branching structures, scattered or clustered in the lung parenchyma. These typically protrude above the surrounding tissue and are easily enucleated [73]. Histologic examination will reveal the presence of numerous angulated and branching osseous structures in the interstitial spaces of the subpleural, interlobular, and interalveolar spaces in DPO. These often have a tubular shape and are found arising from an underlying fibrosing interstitial pneumonitis (Fig. 8.9). Occasionally, the bony spicules project into alveolar lumina, and their intertrabecular spaces often contain fatty marrow elements [60, 61, 66, 73] (Fig. 8.10). Contrary to DPO, NPO consists of nodular proliferations of mature lamellar bone, 1–5 mm in diameter, lying freely within the alveolar spaces and devoid of marrow elements [64, 74] (Fig. 8.11a, b). The surrounding lung parenchyma may be collapsed or fibrotic and contain non-specific inflammatory infiltrates.

8.4.3 Differential Diagnosis

Although the histopathological features of DPO and NPO can be distinguished without difficulty, in some cases, overlapping histological features can be noted, and many of the patients share similar clinical problems (Table 8.1). Other calcifying lesions that can present in the lung include meta-

static pulmonary calcification and a condition termed *alveolar microlithiasis*. The former is characterized by deposition of calcium within the interstitial spaces in a clinical setting of hypercalcemia. This process primarily involves the upper lobe of the lungs and the distribution of the calcium salts follows a more haphazard pattern, generally being deposited in the alveolar walls, bronchial wall, and airways. Contrary to diffuse pulmonary ossification, alveolar microlithiasis is a genetic disorder affecting younger adults. Histologically, the disease is characterized by small, round calcospherites or microliths (250–750 μm in diameter) composed of calcium and phosphorus that primarily fill the alveolar spaces but does not usually involve the interstitium.

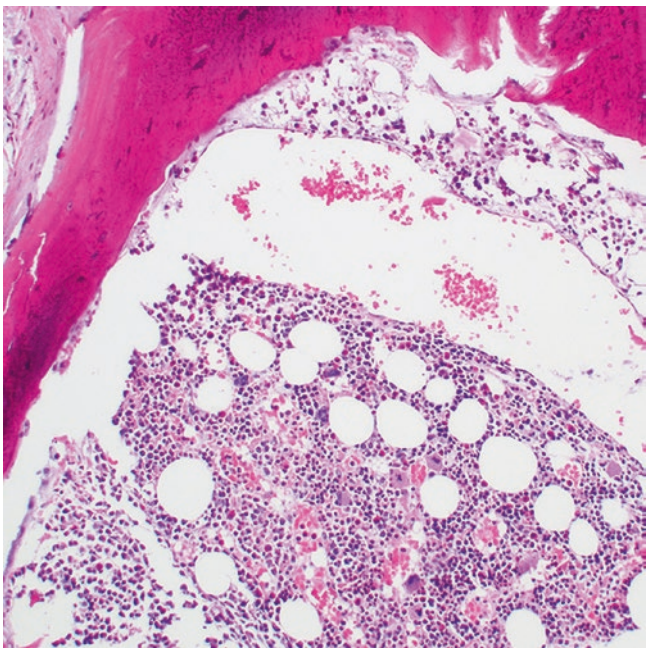

Fig. 8.10 The bone in dendriform pulmonary ossification often contains fatty marrow elements

8.5 Pulmonary Calcification

Pulmonary calcification refers to the deposition of calcium salts in the lung parenchyma as a result of a number of pathologic conditions. This can be broadly divided into two forms: (1) *metastatic pulmonary calcification (MPC)*, which is the result of calcium deposition in normal lung parenchyma, and (2) *dystrophic pulmonary calcification (DPC)*, which occurs when calcification is superimposed on previously injured lung [68] (Table 8.2). The majority of

Table 8.2 Etiology of pulmonary calcification

Metastatic pulmonary calcification	Dystrophic pulmonary calcification
Hypercalcemia:	Ischemia
Chronic renal failure	Trauma
Hyperparathyroidism	Inflammation
Tumor-associated hypercalcemia	Metabolic disturbances
Osteolytic metastases	Infections
Paraneoplastic syndromes	Inhalational injury

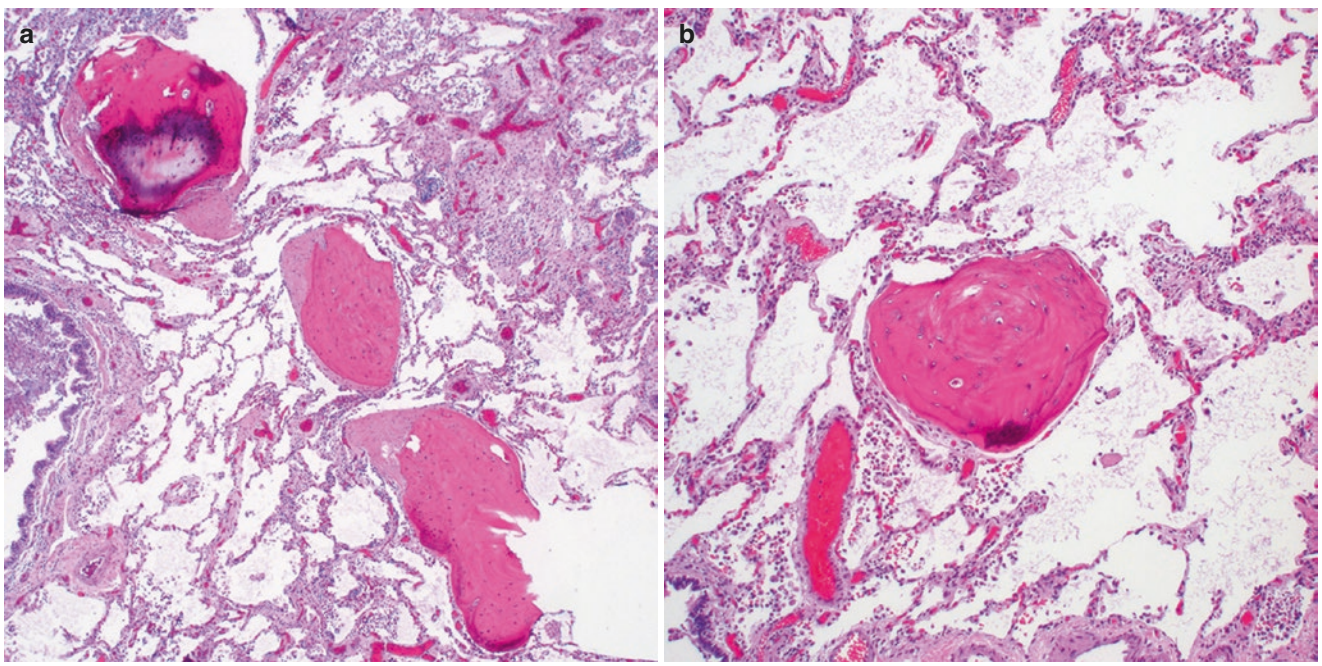

Fig. 8.11 (**a**) Nodular pulmonary ossification shows nodular deposits of mature bone in the alveolar spaces; (**b**) the bony nodules are composed of lamellar bone and are devoid of marrow elements

cases of MPC affect patients with hypercalcemia, particularly those with hyperparathyroidism due to chronic renal failure leading to calcium deposition in various organs [75–77]. The mechanism to cause MPC is not entirely understood but may be influenced by serum calcium and phosphate concentrations, alkaline phosphatase activity, and local physiochemical conditions [68]. Amorphous calcium deposits in necrotic or degenerate tissue in patients with normal calcium metabolism on the other hand are the hallmark of dystrophic calcification [78].

8.5.1 Clinical Features

Pulmonary calcification in MPC and DPC is not an age-related phenomenon but can affect patients of all age groups according to the underlying disorder. MPC is most frequently seen in patients undergoing dialysis for chronic renal failure. Other causes include primary or secondary hyperparathyroidism, hypervitaminosis D, milk-alkali syndrome, or hypercalcemia in patients with hematolymphoid malignancies or bone metastases [78–87]. DPC on the other hand typically follows caseation, necrosis, or fibrosis and may complicate a range of infectious diseases, including histoplasmosis, pneumocystis infection, or tuberculosis as well as amyloidosis, vascular degenerative changes, or tumors [78, 88–90]. The prevalence of MPC in the unselected population is very low but is dramatically increased in hemodialyzed patients, among whom 60–75% were found to be affected by MPC at autopsy [91–93]. Most patients with pulmonary calcification are asymptomatic, and pulmonary function tests are usually normal although, occasionally, restrictive lung function, decreased diffusion capacity, hypoxemia, and respiratory failure can occur [76, 94]. Respiratory symptoms, including dyspnea and non-productive chronic cough, may be further manifestations of the condition, but the degree of calcification usually does not correlate with the extent of the pathology. Chest radiographs are often normal or reveal poorly defined opacities, but calcifications are only seldom evident on the radiograph (Fig. 8.12). High-resolution computed tomography (HRCT) will demonstrate centrilobular ground glass opacities with multiple poorly defined nodules measuring 3–10 mm in diameter or less commonly areas of air space consolidation [95, 96] (Fig. 8.13). Bone scintigraphy can help identify pulmonary calcification in cases where radiographs and HRCT are equivocal [97]. If recognized early, MPC can regress provided that the renal function returns to normal after parathyroidectomy or renal transplantation [98–100]. In general, however, the treatment and prognosis of MPC depends on the underlying condition. In some patients, disease progression with respiratory failure and death has been reported [101, 102].

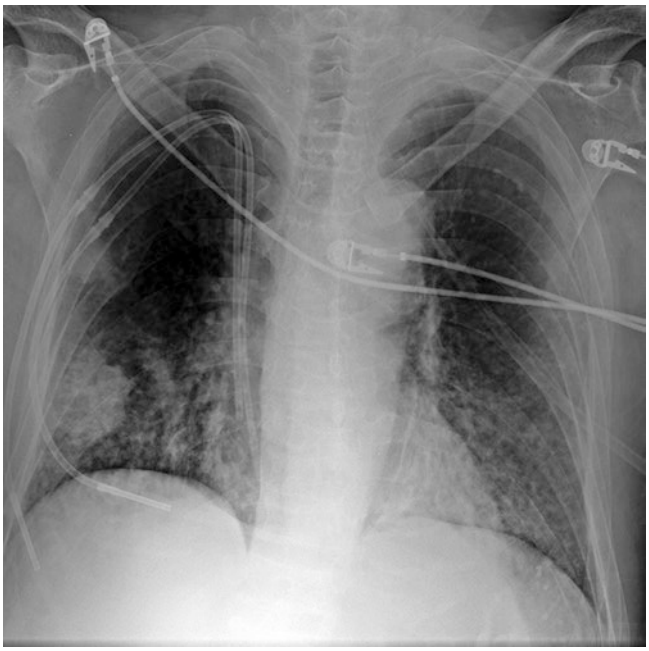

Fig. 8.12 Ill-defined opacities in both lungs are apparent in this chest radiograph of a patient with metastatic pulmonary calcification

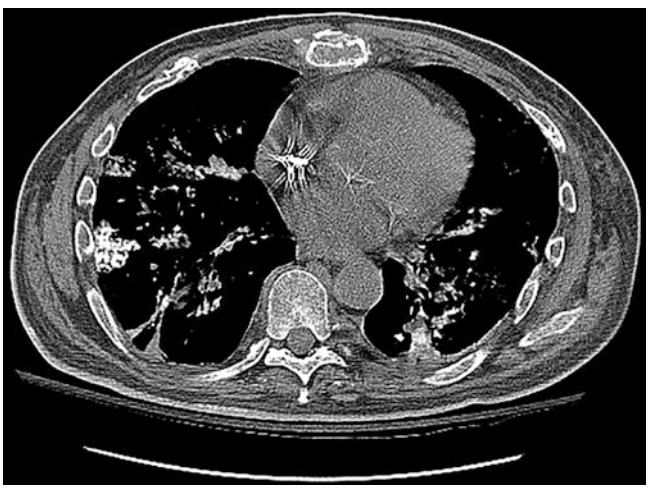

Fig. 8.13 On a computed tomography scan of the chest, metastatic pulmonary calcification is seen as multiple consolidative calcific densities throughout both lungs

8.5.2 Pathological Features

Grossly, the lungs in MPC will display a cut surface that is characterized by numerous yellow-gray spongy nodules measuring up to 0.7 cm in diameter [91]. Typically, the lungs will be involved in an asymmetric and bilateral pattern [78]. Histologically, the process is restricted to the interstitial spaces and shows deposition of deeply basophilic granular or linear calcium in the walls of the alveoli leading to alveolar rigidity (Fig. 8.14a–c). The calcification appears to have a particular affinity for elastic tissue and can also be seen in the

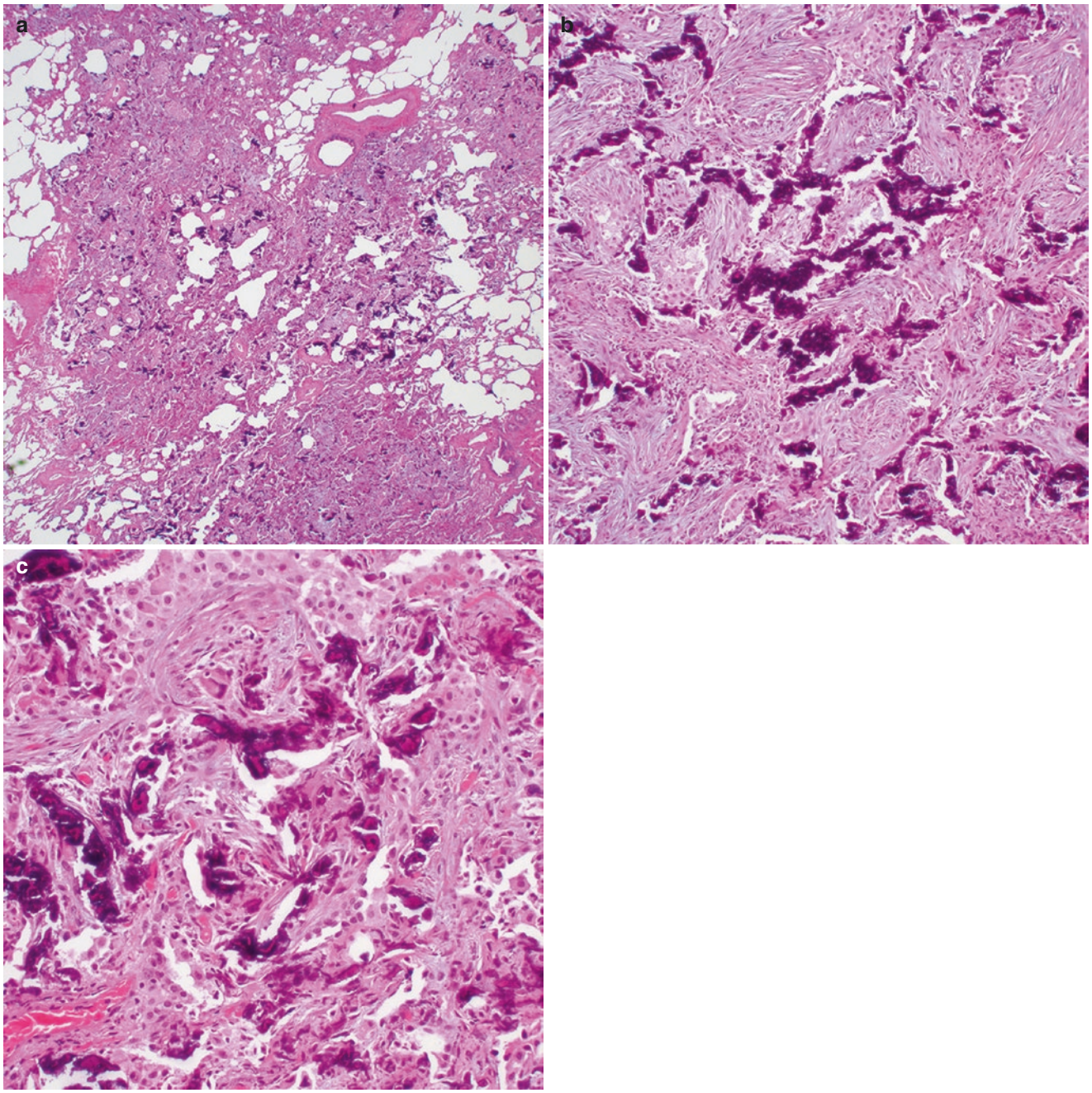

Fig. 8.14 (**a**) Low power magnification of metastatic pulmonary calcification shows deposition of eosinophilic granular and calcified material in the interstitial spaces of the lung parenchyma; (**b**) the calcifications often have a linear shape and are (**c**) distributed along the alveolar walls

walls of small vessels, bronchi, and bronchioles [78, 91] (Fig. 8.15a, b). In contrast, the calcifications in DPC can show variable gross and microscopic patterns depending on the underlying etiologic cause and can range from plate-like, elongated, or shell-shaped calcifications in pneumocystis pneumonia [78] to interstitial calcium deposits in the subpleural regions in the lower zones of the lung in amyloidosis [68] (Fig. 8.16).

8.5.3 Differential Diagnosis

Distinction of MPC from DPC should be relatively straightforward taking into account the clinical setting and histological pattern of the disease. MPC almost exclusively occurs against a background of hypercalcemia due to various clinical causes. Contrary to that, DPC is unrelated to such setting and primarily occurs as a result of tissue injury. Similarly, the

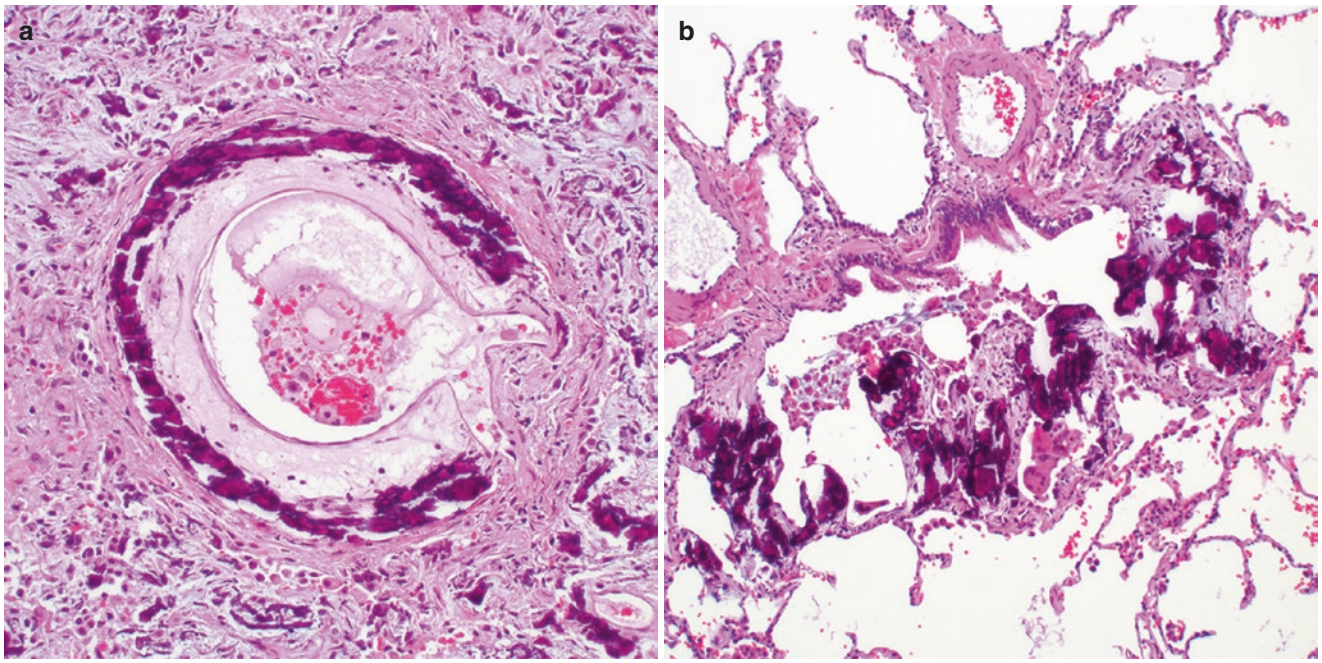

Fig. 8.15 (**a**) The calcific deposits in metastatic pulmonary calcification often show a strong affinity for blood vessels or (**b**) small airways

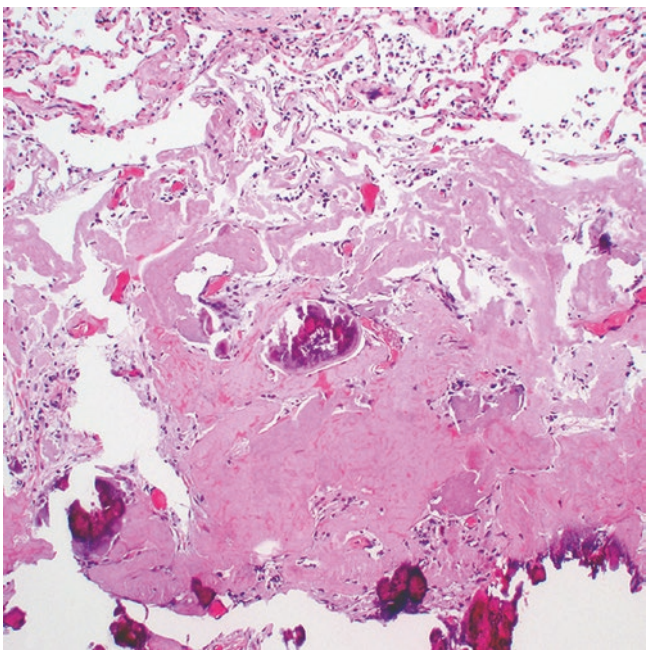

Fig. 8.16 Dystrophic pulmonary calcification is seen superimposed on previously injured lung parenchyma, here in a case of pulmonary amyloidosis

histological pattern in MPC often shows bilateral lung involvement with predilection of the upper zones, while in DPC, the pattern of calcium deposition is much more variable and largely depends on the distribution of the underlying necrotizing or degenerative process. As mentioned above, alveolar microlithiasis, another calcifying process of the lungs, is a genetic disorder producing small concentric calcospherites that get deposited in the alveolar spaces. This disorder can be separated from diffuse pulmonary calcification based on the different clinical setting, disease pattern, and histological characteristics.

8.6 Pulmonary Hyalinizing Granuloma

Pulmonary hyalinizing granuloma (PHG) is a rare lesion of the lung that was first characterized by Engleman et al. in 1977 [103]. Since then less than 150 cases have been reported in the medical literature [104]. It is an unusual fibrosing lesion that presents as solitary or multiple lung nodules radiologically closely mimicking metastatic carcinoma. The final diagnosis therefore heavily relies on histologic analysis. The pathogenesis for this condition is still unclear; however, the strong association with inflammatory, autoimmune, and hematologic diseases is suggestive of an underlying immunologic pathway [104] (Table 8.3). Moreover, it has been speculated that PHG may represent a lesion in the spectrum of IgG4-related disease due to frequent occurrence with systemic fibrosis and detection of elevated serum and tissue IgG4 in some cases [105].

8.6.1 Clinical Features

PHG primarily affects the adult population with an age range from 15 to 83 years and a mean age at diagnosis of 45 years.

Table 8.3 Diseases commonly associated with pulmonary hyalinizing granuloma

Autoimmune diseases	Infectious diseases	Fibrosing lesions
Idiopathic thrombocytopenic purpura Sarcoidosis Rheumatoid arthritis Grave disease Hashimoto disease Sjögren disease Riedel thyroiditis Multiple sclerosis Granulomatosis with polyangiitis IgA nephropathy Cutaneous vasculitis	Tuberculosis Histoplasmosis	Retroperitoneal fibrosis Mediastinal fibrosis IgG4 disease

Ig immunoglobulin

Fig. 8.17 Computed tomography scan of the chest of a patient with pulmonary hyalinizing granuloma shows a well-circumscribed solitary lesion in the central left lung

There is slight male predilection and around 60% of patients are active smokers. Patients most often present with respiratory symptoms, including cough, dyspnea, and hemoptysis or general symptoms, such as fever, weight loss, and night sweats. It is also not uncommon for patients to be entirely asymptomatic, and their lesions are found during diagnostic imaging for unrelated reasons. As mentioned above, there is a frequent association with systemic diseases, including systemic fibrosis, infectious diseases, autoimmune diseases, and hematological disorders [103–107] (Table 8.3). Radiologic imaging usually shows randomly distributed nodules and masses that may be solitary or multiple. Typically, the lesions are well circumscribed and range in size from a few millimeters to 15 cm in diameter (Fig. 8.17). Calcification and cavitary changes are only rarely seen [103, 104, 108]. On PET-CT scan the lesions may be hypermetabolic simulating a malignant process [107, 109]. The prognosis for patients with PHG is generally considered excellent in keeping with the benign nature of the lesions [104]; however, in some cases, progressive enlargement of the nodules has been described [103]. There is no specific treatment for PHG although corticosteroids have been shown to improve the natural evolution of the process. For most patients, however, close clinical follow-up is usually all that is required.

8.6.2 Pathological Features

Gross examination of PHG reveals discrete pulmonary nodules of firm texture and pearly white to translucent color. The nodules are typically well circumscribed but not encapsulated. Calcification or ossification are not a typical features of PHG [103]. Microscopically, PHG are composed of homogeneous eosinophilic hyaline collagen bundles organized in a lamellar or coarse storiform pattern and often arranged around blood vessels in a concentric fashion (Fig. 8.18a–c). Collections of lymphocytes, plasma cells, and histiocytes are often found in the periphery of the nodules (Fig. 8.19); eosinophils and giant cells may also be noted occasionally. Foci of ischemic necrosis may be seen but are not invariably present. Of note, the lesions may also display intimal fibrosis or medial hyalinization of associated blood vessels [103–107].

8.6.3 Histochemical and Ultrastructural Features

Histochemical stains for acid-fast bacilli and fungal organisms are negative. Although usually negative for a Congo red stain, isolated cases may show a focal positive reaction, including apple green birefringence under polarized light [103, 106, 107]. Contrary to the fibrillary structure of amyloid, PHG is composed of electron-dense, compact, homogeneous, and amorphous material on electron microscopy [110].

8.6.4 Differential Diagnosis

The hypocellular pattern of PHG is reminiscent of a range of lesions with similar histological appearance. Infectious granulomas, especially when hyalinized, may closely mimic PHG. PHG can be distinguished from granulomatous inflammation based on its distinctive lamellar and concentric pattern and negative histochemical stains for infectious organisms. Another entity that enters the differential diagnosis is inflammatory pseudotumor (IPT) of the lung, more specifically the plasma cell type (plasma cell granuloma).

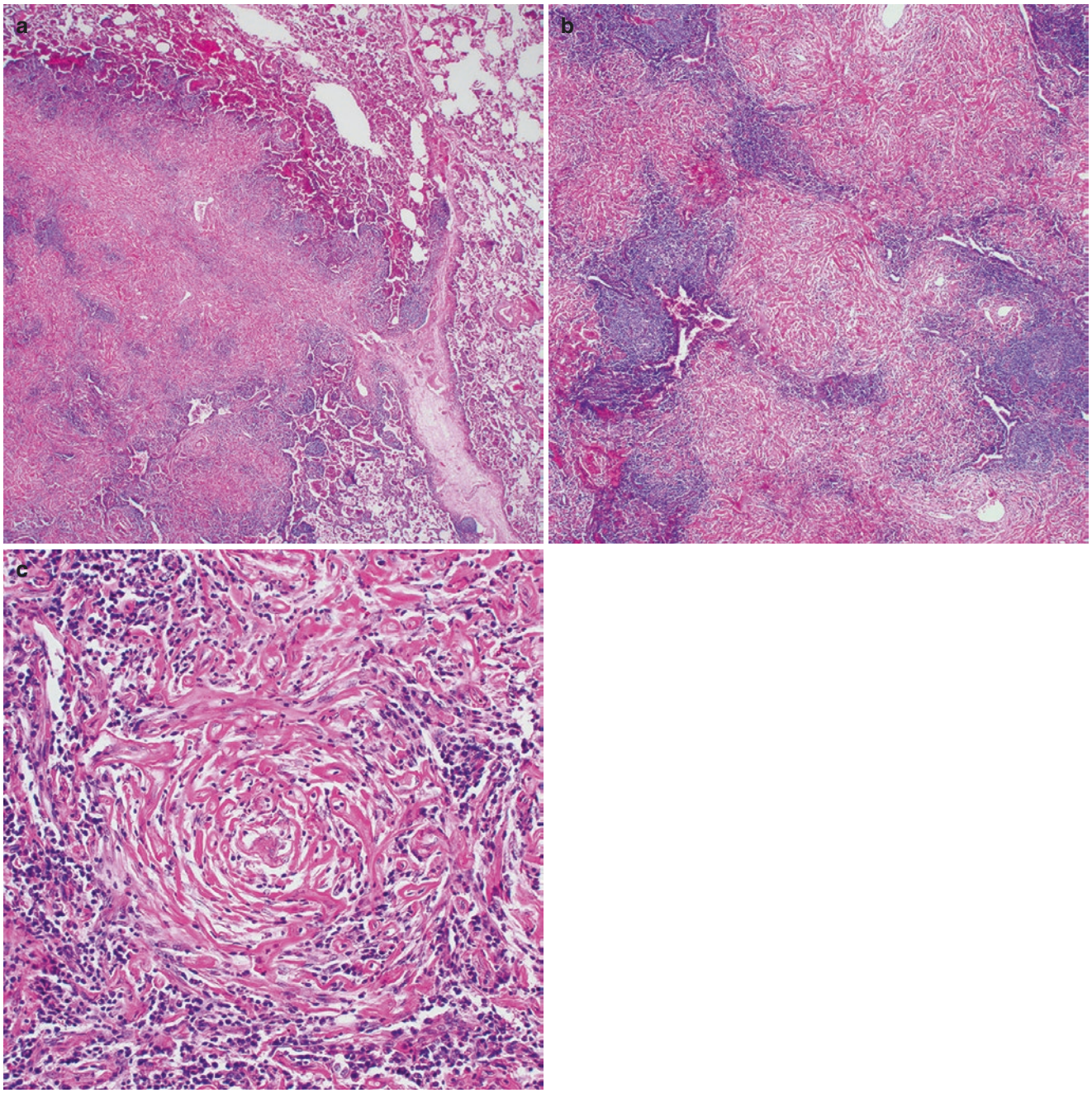

Fig. 8.18 (**a**) Low power view of a pulmonary hyalinizing granuloma shows a well-circumscribed lesion affecting the lung parenchyma; (**b**) the lesion is characterized by nodular or storiform deposits of collagen bundles; (**c**) the collagen is often arranged in a concentric pattern around small blood vessels

Contrary to PHG, IPT typically occur in a younger patient population and are usually solitary lesions. In addition, they usually show a diffuse distribution of numerous plasma cells and fibroblasts unlike the hypocellular appearance of PHG. Further diagnostic considerations include the nodular types of amyloidosis and light chain deposition disease (LCDD) of the lung. Both these conditions consist of one or more nodular deposits of pink, amorphous material in the lung parenchyma. In contrast to PHG, the nodular deposits of amyloidosis and LCDD are often accompanied or admixed with giant cells as well as foci of calcification or ossification. In addition, these conditions lack the characteristic storiform or concentric pattern of PHG.

8.7 Pulmonary Amyloidosis

Amyloidosis refers to a group of diseases characterized by the deposition of insoluble proteins in the extracellular matrix of tissues and organs with the potential of causing

significant organ dysfunction and death [111]. The term *amyloid* (starch-like) to describe this process was first introduced to the literature by Rudolf Virchow when he recognized deposition of a substance in the brain that had starch-like staining properties [112]. Today, the term amyloid is applied to a wide group of misfolded autologous proteins that deposit in tissues in the form of fibrils [111]. Amyloidosis can be a systemic process or present as localized disease. Currently, almost 15 different forms of systemic amyloidosis are recognized and classified according to their different precursor proteins [113]. Since treatment and prognosis of these various forms of amyloidosis can differ, detailed identification of the exact type as well as extent of the disease (systemic versus localized) is critical [111]. The most common forms of amyloidosis include *systemic AL*, *systemic AA*, *systemic wild-type ATTR*, *systemic hereditary ATTR*, and *localized AL amyloidosis* (Table 8.4). The lungs are frequently involved in systemic amyloidosis but can also be the site of localized disease. Furthermore, amyloidosis affecting the lung can be divided into three separate forms depending on the disease pattern: *diffuse alveolar-septal amyloidosis (DASA)*, *nodular pulmonary amyloidosis (NPA)*, and *tracheobronchial amyloidosis (TBA)* (Table 8.5). DASA is characterized by amyloid deposition in the walls of alveolar septa and blood vessels and is most often a manifestation of systemic AL amyloidosis. Localized forms and associations with other types of systemic amyloidosis have also been described [114–117]. Contrary to that, NPA is defined as one or more nodule-forming amyloid deposits involving the lungs. It is generally associated with localized AL or AL/AH (mixed immunoglobulin light and heavy chain) amyloidosis although rarely cases of systemic amyloidosis have also been reported [118–124]. In addition, recent studies have suggested that most cases of NPA are the result of an underlying low-grade lymphoproliferative disorder in the spectrum of extranodal marginal zone lymphoma of mucosa-associated lymphoid tissue (MALT lymphoma) [118]. Lastly, TBA refers to amyloid deposition in the tracheobronchial tree, either in a plaque-like or nodular fashion. Most cases appear to represent localized AL amyloidosis, but as with the other forms of pulmonary amyloidosis, rare cases associated with systemic amyloidosis, most commonly AL and AA amyloidosis, have been recognized [114, 125–130] (Table 8.5).

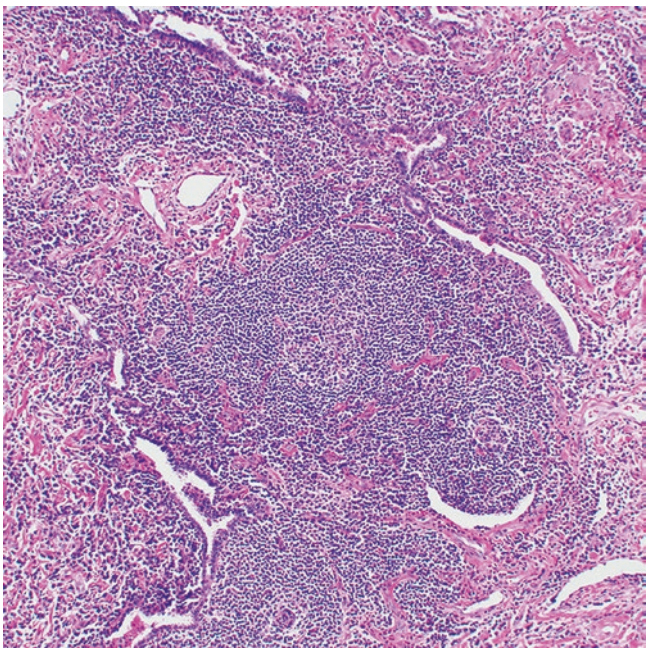

Fig. 8.19 The periphery of the collagenous nodules in pulmonary hyalinizing granuloma typically contains an inflammatory cell infiltrate, including lymphocytes, plasma cells, and histiocytes

8.7.1 Clinical Features

Because of its rare symptomatology and common association with systemic amyloidosis, *DASA* most often comes to the attention of the pathologist at autopsy, and the patients'

Table 8.5 Subtypes of pulmonary amyloidosis

	Diffuse alveolar septal amyloidosis	Nodular amyloidosis	Tracheobronchial amyloidosis
Age	7th decade	7th decade	5th–6th decade
Sex ratio	M = F	M > F	M = F
Underlying condition	Systemic amyloidosis	Localized AL amyloidosis	Localized AL amyloidosis
Treatment	Based on underlying systemic amyloidosis	Conservative surgical excision	Laser or forceps debridement, external beam radiation
Prognosis	Guarded; depends on effects of systemic disease on other organ systems	Excellent	Guarded; 30% mortality

Table 8.4 Common forms of amyloidosis

Current nomenclature	Previous nomenclature	Precursor protein	Underlying condition
Systemic AL amyloidosis	Primary amyloidosis	Immunoglobulin light chain	Plasma cell dyscrasia
Systemic AA amyloidosis	Secondary amyloidosis	(Apo) serum amyloid A	Chronic inflammatory conditions
Systemic wild-type ATTR amyloidosis	Senile systemic amyloidosis	Transthyretin, wild-type	Age-related
Systemic hereditary ATTR amyloidosis	Familial amyloid polyneuropathy	Transthyretin, mutated type	Mutations in *transthyretin* gene
Localized amyloidosis	–	Immunoglobulin light chain	MALT lymphoma

MALT mucosa-associated lymphoid tissue, *ATTR* transthyretin amyloidosis

symptoms are usually related to the effects of amyloid deposition in other organ systems. Affected patients are predominantly elderly men, and symptoms are non-specific, including fatigue and weight loss [131]. As the disease progresses, progressive interstitial lung disease with respiratory compromise may develop, and pulmonary function tests can show a restrictive pattern with reduced diffusion capacity and hypoxemia. Radiologic imaging will display reticular or reticulonodular patterns of lung involvement on chest radiography or computed tomography (CT) scans; pleural effusions are also common [125] (Fig. 8.20). The treatment of DASA is primarily aimed at treating the underlying systemic amyloidosis, including chemotherapy and autologous stems cell transplantation for systemic AL amyloidosis [132] or colchicine for systemic AA amyloidosis [133]. Such strategies are contraindicated for systemic wild-type and hereditary ATTR amyloidosis which require different approaches such as liver transplantation in the latter [134]. Likewise, the prognosis for patients with DASA largely depends on the effects of the disease on other organ systems, most importantly the heart, while DASA itself is only infrequently associated with an immediate effect on survival [135]. The nodules of *NPA* are usually solitary lesions that are incidentally detected during imaging procedures for unrelated reasons. The mean age of patients is 67 years, and males are more commonly affected than females (ratio 3:2) [114, 136]. On chest imaging, the nodules of NPA are well circumscribed and range in size from 0.6 to 9.0 cm. They are often located in a subpleural location in the lower lobes of the lung (Fig. 8.21). Calcification and cavitation can be seen in a subset of cases [125, 137–139] (Fig. 8.22). Because of the localized nature of NPA, conservative surgical resection is usually curative and the long-term prognosis is excellent [140]. *TBA* is the least common form of pulmonary amyloidosis with a peak incidence in the 5th to 6th decade and no specific sex predilection [125, 127, 141]. Dyspnea, cough, hemoptysis, and hoarseness are the most common symptoms and typically related to the degree of airflow obstruction (Fig. 8.23). CT scanning of the chest will show thickening of the major

Fig. 8.21 Several irregular nodular lesions affecting both lungs are seen on this computed tomography scan of the chest in a patient with nodular pulmonary amyloidosis

Fig. 8.20 Computed tomography scan of a patient with diffuse alveolar-septal pulmonary amyloidosis shows bilateral pleural effusions

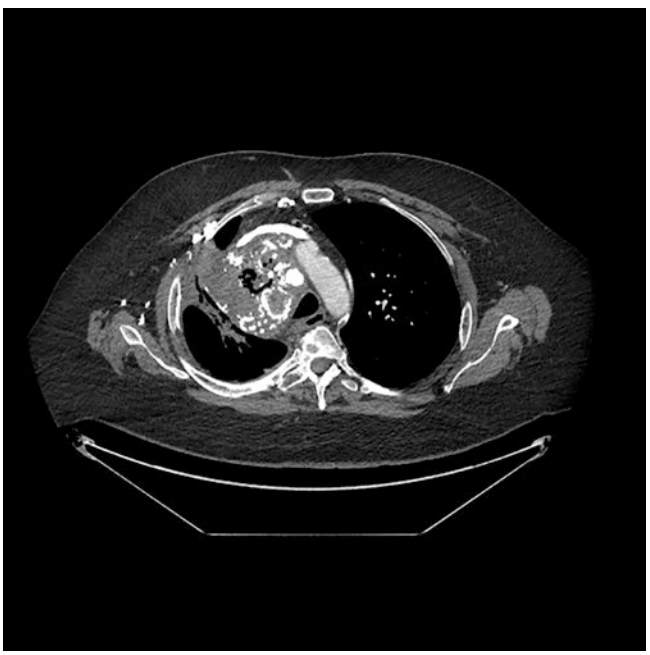

Fig. 8.22 A large mass-like lesion with cavitation and calcification in the right upper lobe of a patient with nodular pulmonary amyloidosis on a computed tomography scan

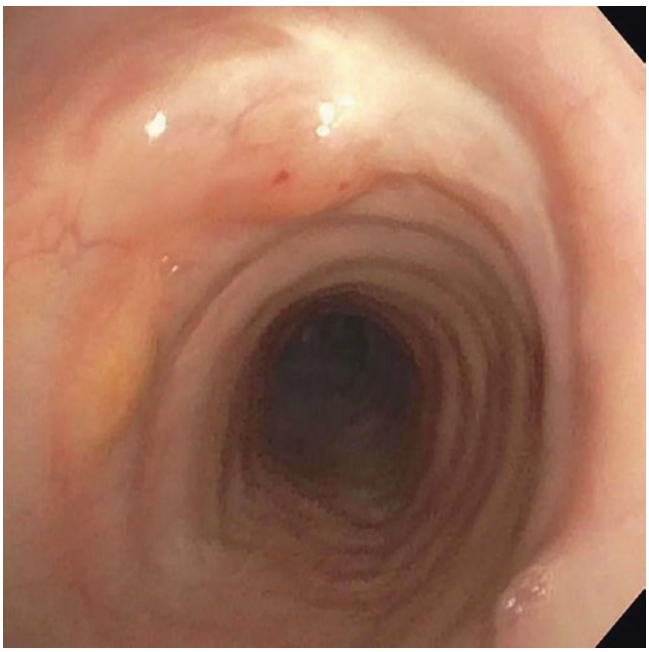

Fig. 8.23 Submucosal nodularity in the tracheobronchial tract of a patient with the tracheobronchial form of amyloidosis

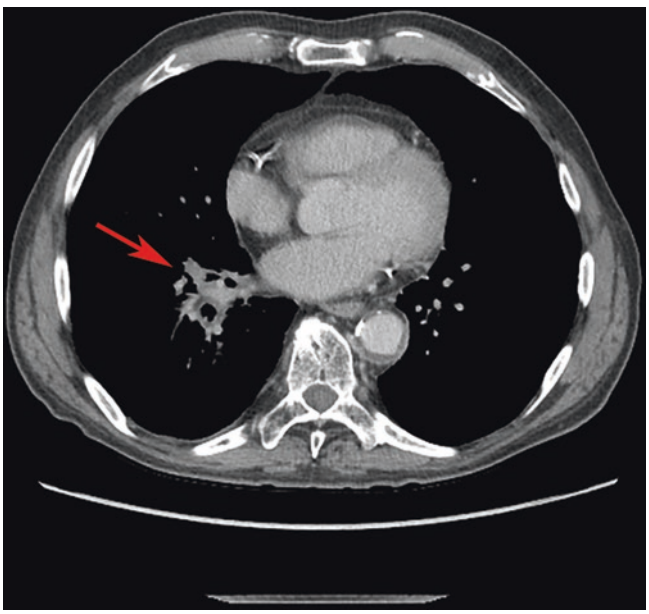

Fig. 8.24 Computed tomography scan of a patient with tracheobronchial amyloidosis shows narrowing of the central bronchial tree (arrow) in the right hilar/perihilar area

airways, irregular narrowing of the airway lumen, and heterotopic calcification of the airway walls [127, 134, 142, 143] (Fig. 8.24). The treatment of TBA usually consists of laser or forceps debridement or external beam radiation. Despite this, recurrence is common, and about a third of patients eventually succumb to the disease [127, 144].

8.7.2 Pathological Features

Lungs with *DASA* will demonstrate a rubbery and sponge-like consistency involving all lobes on gross examination. The pleura may also be involved by the process which may lead to recurrent pleural effusions [140]. Low power microscopic examination shows a seemingly preserved lung architecture, but higher magnification will reveal diffuse deposition of acellular eosinophilic material in the alveolar septa, vessel walls, and adjacent visceral pleura (Fig. 8.25a–c). The material may also form small interstitial or larger confluent nodules (Fig. 8.26). The lesions are typically acellular and only rarely accompanied by plasma cells or giant cells [125, 140]. Gross examination of the lungs in NPA will show solitary or multiple nodular masses in the lung parenchyma, measuring 0.6–9.0 cm in size and demonstrating a waxy, gray-tan, and rubbery cut surface. On microscopic examination, the nodules (also called *amyloidomas*) are well demarcated and composed of brightly eosinophilic and acellular material with small aggregates of plasma cells or lymphocytes in the periphery (Fig. 8.27a–c). The nodules often show evidence of calcification or ossification, and giant cells are commonly identified [125, 140] (Fig. 8.28a, b). Submucosal soft tissue masses narrowing the airways and compromising the airway lumen can be seen on gross examination of the lungs in *TBA*. Microscopically, homogeneous eosinophilic material is seen in the submucosa of the airways either in the form of diffuse plaque or sheet-like masses or as nodular deposits (Fig. 8.29a–c). The vessel walls of small submucosal vessels are commonly affected, and plasma cells, giant cells, calcifications, and ossification are a common finding [125, 140] (Fig. 8.30).

8.7.3 Laboratory, Histochemical, Immunohistochemical, and Other Ancillary Investigations

The vast majority of patients with systemic AL amyloidosis often contain monoclonal immunoglobulins or free light chains in their serum or urine [145]. λ light chains are more commonly detected than κ light chains in systemic AL amyloidosis, DASA, and TBA [140], while the opposite has been reported for NPA [118]. The presence of amyloid in tissue sections can be confirmed using a Congo red histochemical stain which will highlight the bright orange-red deposits with bright-field microscopy (Fig. 8.31a, b). Furthermore, under polarized light, an apple-green birefringence is typically displayed and is currently considered the gold standard in the identification of amyloid in tissue sections (Fig. 8.32a, b). Other histochemical staining methods include methyl violet which will show a metachromatic reaction and thioflavin T [146]. Ultrastructural examination will reveal

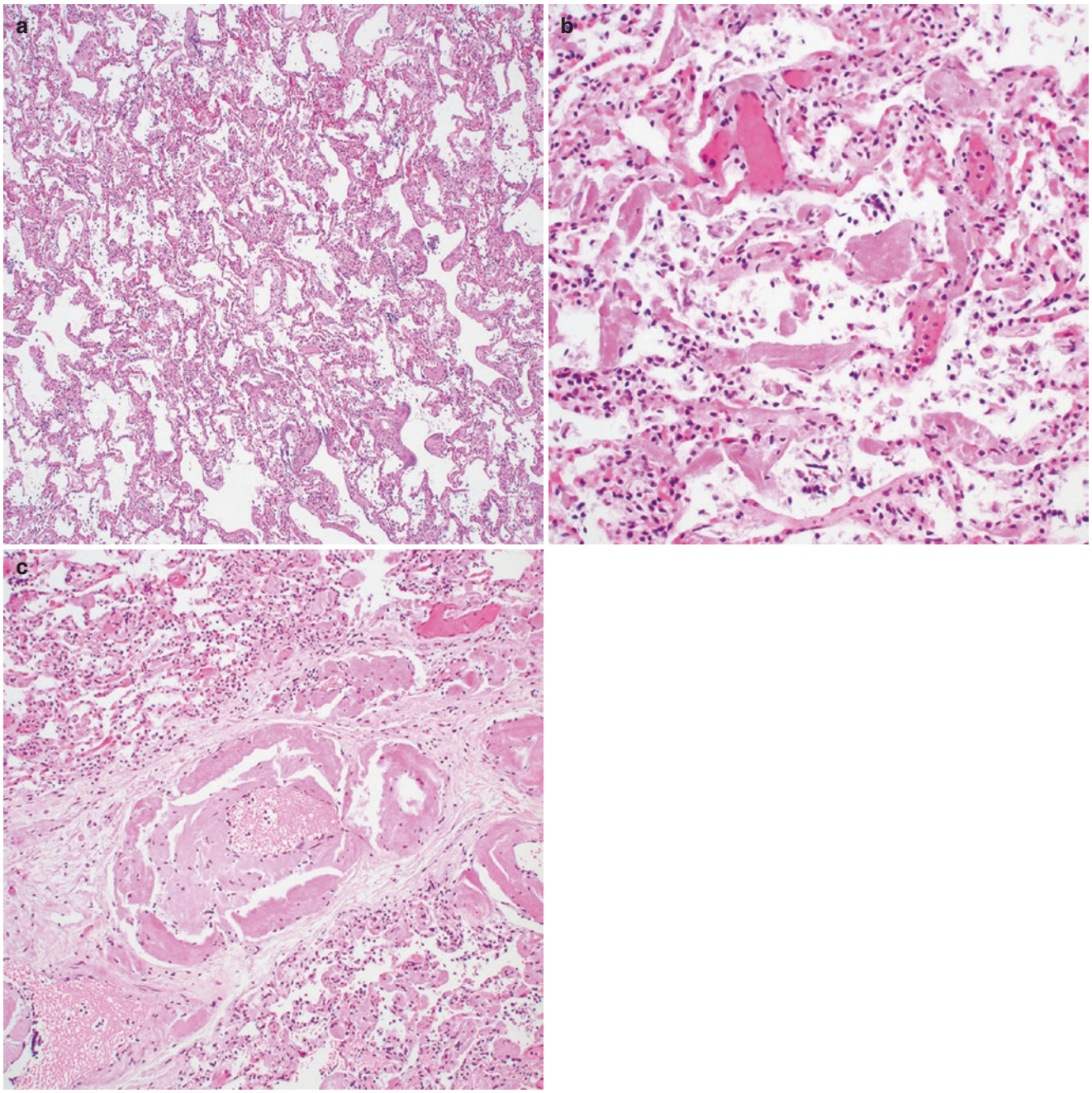

Fig. 8.25 (**a**) The lung architecture in diffuse alveolar-septal pulmonary amyloidosis appears preserved on low power magnification; (**b**) higher magnification shows subtle thickening of the alveolar septa and (**c**) vessel walls by an amorphous eosinophilic material

haphazardly arranged non-branching fibrils measuring 8–10 μm in diameter [147] (Fig. 8.33). Since the treatment and prognosis of amyloidosis heavily depends on the fibril protein, precise identification of the amyloid subtype is strongly recommended [111]. Although immunohistochemical antibodies are available for major amyloid subtypes (κ and λ light chains, serum amyloid A, and transthyretin), the classification of amyloid by this method is suboptimal due to abundant background staining, and mass spectrometry-based proteomic analysis is currently the preferred method of amyloid subtyping in biopsy specimens [148].

8.7.4 Differential Diagnosis

The differential diagnosis for pulmonary amyloidosis largely depends on the pattern of disease affecting the lung. The interstitial pattern of deposition associated with *DASA*

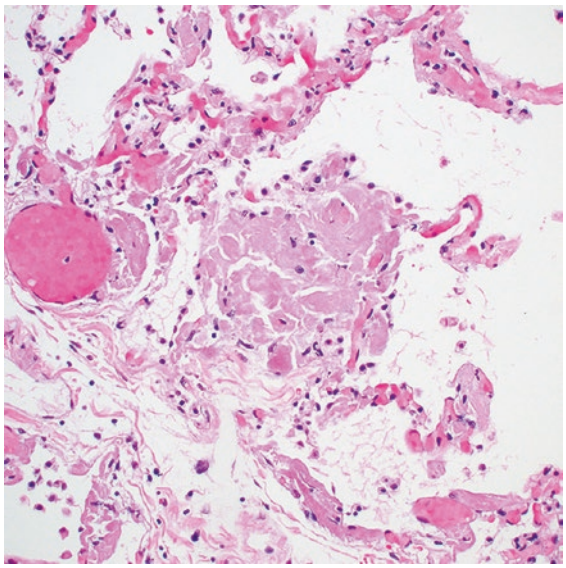

Fig. 8.26 Small nodular amyloid deposit in a case of diffuse alveolar-septal pulmonary amyloidosis

can be confused with interstitial lung disease, such as usual interstitial pneumonitis (UIP) or non-specific interstitial pneumonitis (NSIP). The glassy acellular appearance of the amyloid deposits coupled with a positive Congo red stain should be sufficient to distinguish between these entities. Pulmonary hyalinizing granuloma (PHG) is a lesion that can closely resemble NPA based on its clinical and radiological appearance as asymptomatic solitary or multiple pulmonary nodules. Histologically, PHG differs from amyloid nodules due to the presence of thick collagen bundles arranged in a lamellar fashion. Calcification or osseous metaplasia are not associated with this entity, and Congo red staining will deliver a negative result. Pulmonary light chain deposition disease (LCDD) is another entity that can closely mimic pulmonary amyloidosis and that typically presents with diffuse interstitial or nodular tissue deposits (Table 8.6). LCDD can be clinically and histologically indistinguishable from pulmonary amyloidosis, and separation of the disease processes usually requires application of

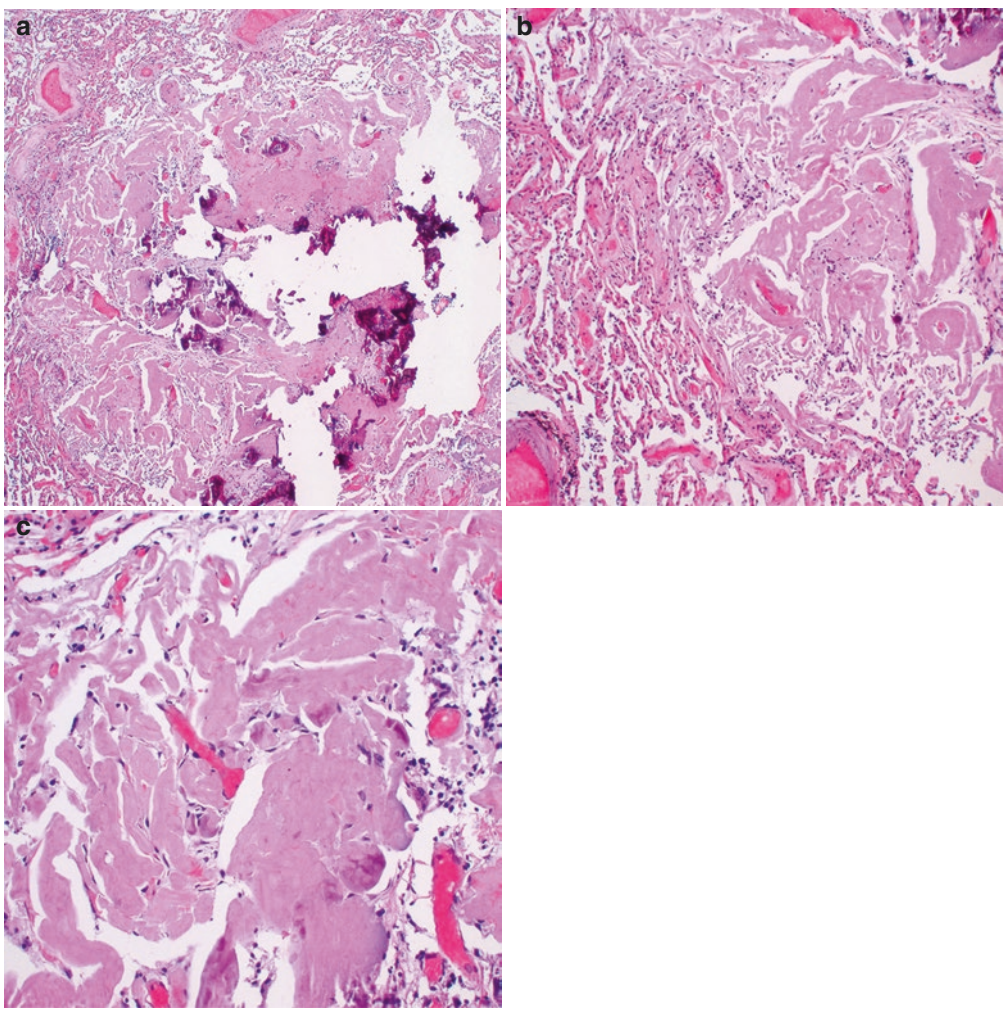

Fig. 8.27 (**a**, **b**) Low power view of an amyloidoma of the lung demonstrates a circumscribed lesion within the lung parenchyma; (**c**) the deposit is composed of brightly eosinophilic and acellular material

ancillary techniques. In this context, amyloidosis differs from LCDD by a positive reaction with a Congo red stain and fibrillary quality of the protein deposits on ultrastructural examination, contrary to the negative reaction with Congo red and granular ultrastructural appearance of LCDD.

8.8 Pulmonary Light Chain Deposition Disease

Light chain deposition disease (LCDD) is a rare condition characterized by deposition of non-amyloid immunoglobulin light chains in various organs interfering with their normal

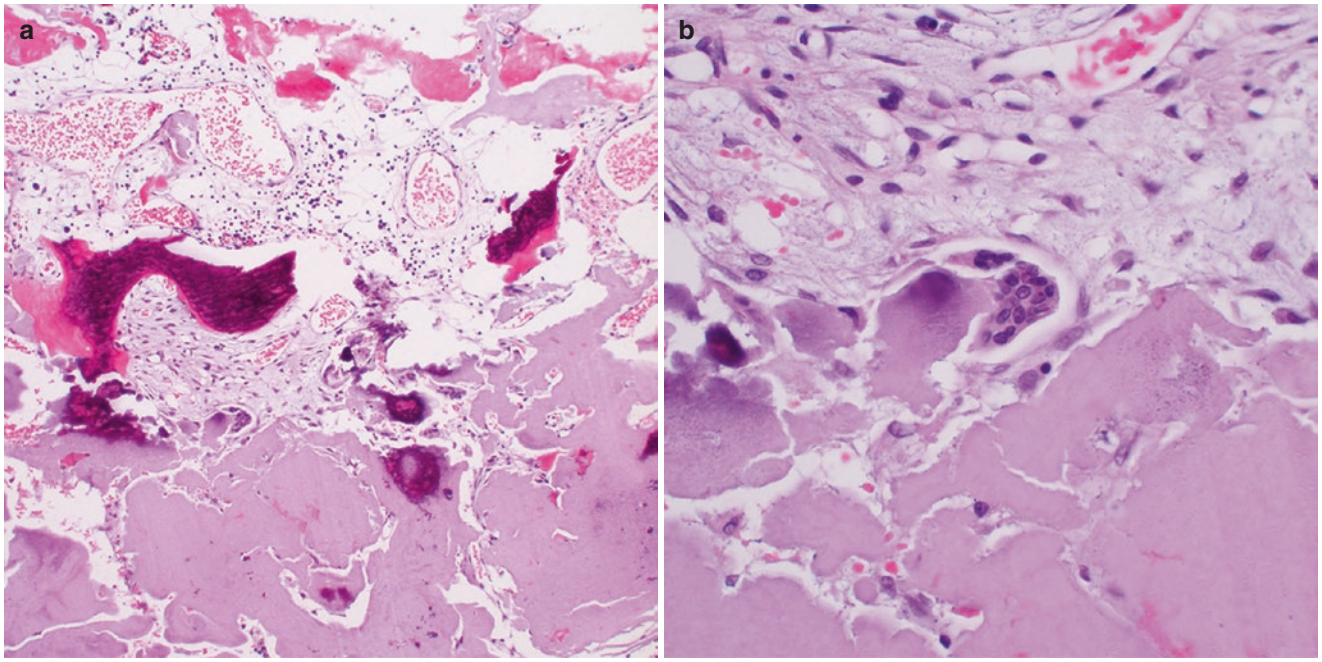

Fig. 8.28 (**a**) Areas of calcification and ossification and (**b**) multinucleated giant cells are frequent findings in the nodular form of pulmonary amyloidosis

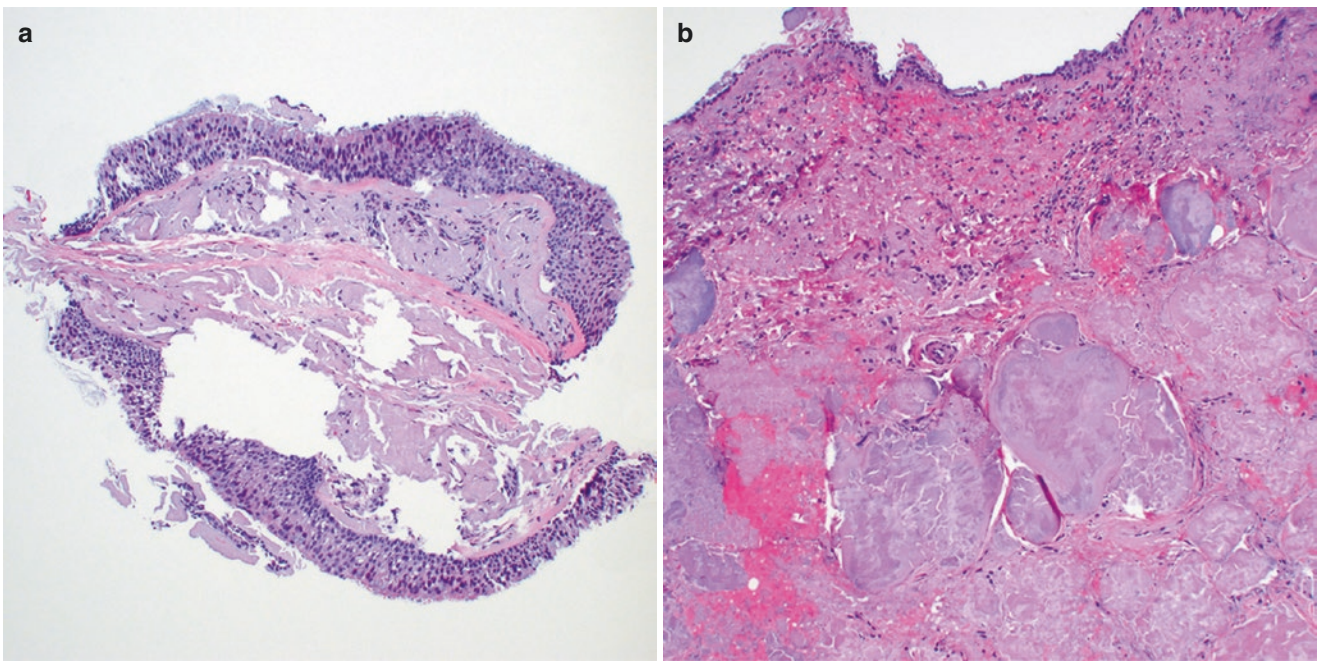

Fig. 8.29 (**a**) In tracheobronchial amyloidosis, the deposits are typically located in the submucosa of the airways; (**b**) the deposits are homogeneous and often brightly eosinophilic; (**c**) entrapped normal airway components (here bronchial gland) may be identified in some cases

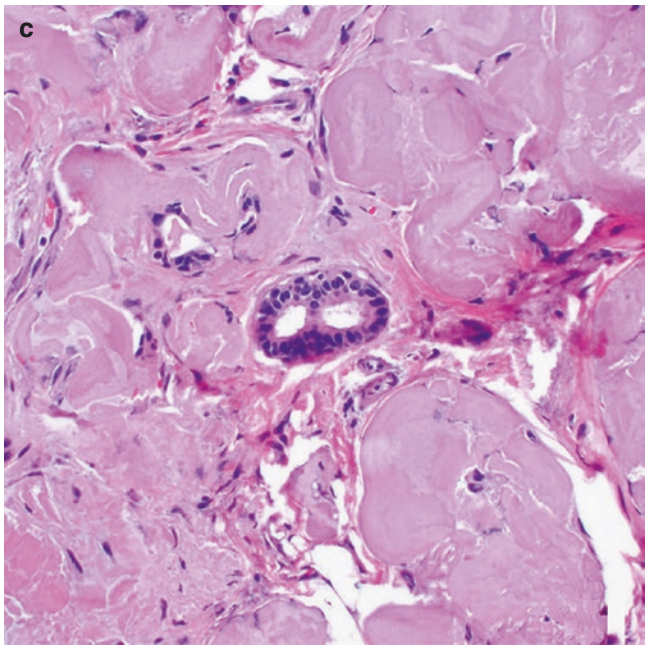

Fig. 8.29 (continued)

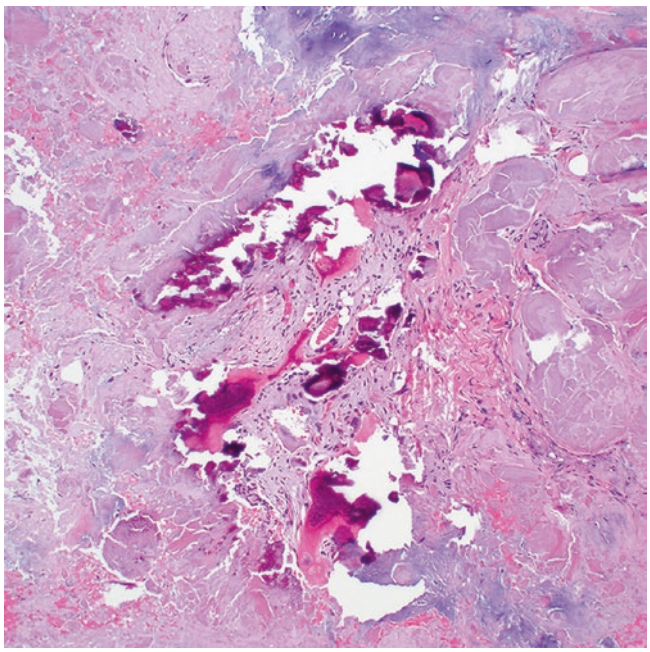

Fig. 8.30 Like other forms of amyloidosis, the tracheobronchial type can be associated with areas of calcification and ossification

function. It is most commonly seen in patients with lymphoproliferative disease or autoimmune disorders but can be idiopathic [149, 150]. LCDD is primarily a multisystem disease with kidney, liver, and heart involvement being the most common manifestations. The lungs are only rarely involved, either as part of systemic disease or in a localized fashion [145, 149]. Histologically, LCDD is characterized by amorphous tissue deposits just like amyloidosis, and both conditions share similar pathogenesis and clinical findings. Contrary to amyloidosis, however, the deposits of LCDD are not congophilic, fail to reveal apple-green birefringence under polarized light, and form granular, not fibrillary, deposits when examined ultrastructurally (Table 8.6). On the other hand, pulmonary involvement of LCDD can present in two patterns, nodular and diffuse, once again sharing similarities with amyloidosis. Ultimately, electron microscopy and/or liquid chromatography-mass spectrometry may be necessary to distinguish the two conditions (Table 8.6).

8.8.1 Clinical Features

LCDD can occur over a wide age range (35–76 years) and is more prevalent in men [149]. Since most cases of pulmonary LCDD occur in a setting of systemic disease, renal and/or cardiac involvement is usually present and characterized by renal or congestive cardiac failure. In addition, many cases of LCDD occur in association with plasma cell dyscrasia, especially multiple myeloma, although an association with other B cell disorders, such as lymphoma, Waldenström macroglobulinemia, and chronic lymphocytic leukemia, has also been reported [151]. Pulmonary involvement may be an incidental finding, or patients may present with dyspnea, cough, and rarely respiratory failure [145, 149, 151–155]. Radiologic imaging will demonstrate solitary or multiple pulmonary nodules on average measuring 1.0 cm in diameter (range, 0.4–1.5 cm) that can contain calcifications or cavitations. The presence of thin-walled pulmonary cysts or bullous cavities has also been noted [145, 156]. Bilateral interstitial reticulonodular infiltrates are typically seen in the diffuse form of pulmonary LCDD [157]. Patients with nodular pulmonary LCDD generally have a good prognosis, and conservative treatment approaches, such as corticosteroids, methotrexate, or rituximab, or observation usually lead to successful management of the disease [145, 156, 158]. The prognosis for patients with the diffuse form of pulmonary LCDD is more guarded and characterized by frequent renal failure and associated mortality, despite treatment with corticosteroids, cytotoxic medications, and even lung transplantation [145, 157].

8.8.2 Pathological Features

Macroscopically, the lung parenchyma with pulmonary LCDD feels firm to touch. The cut surface of lungs with the diffuse form of LCDD is firm, rubbery, and dry and may show diffusely scattered minute nodules in a peribronchial or perivascular distribution. The parenchyma of the nodular form contains solitary or multiple small nodules of tan or gray color ranging in size from several millimeters to 3.2 cm [145, 156]. Microscopic examination reveals deposits of amorphous acellular and eosinophilic material in the alveolar septa and vessel

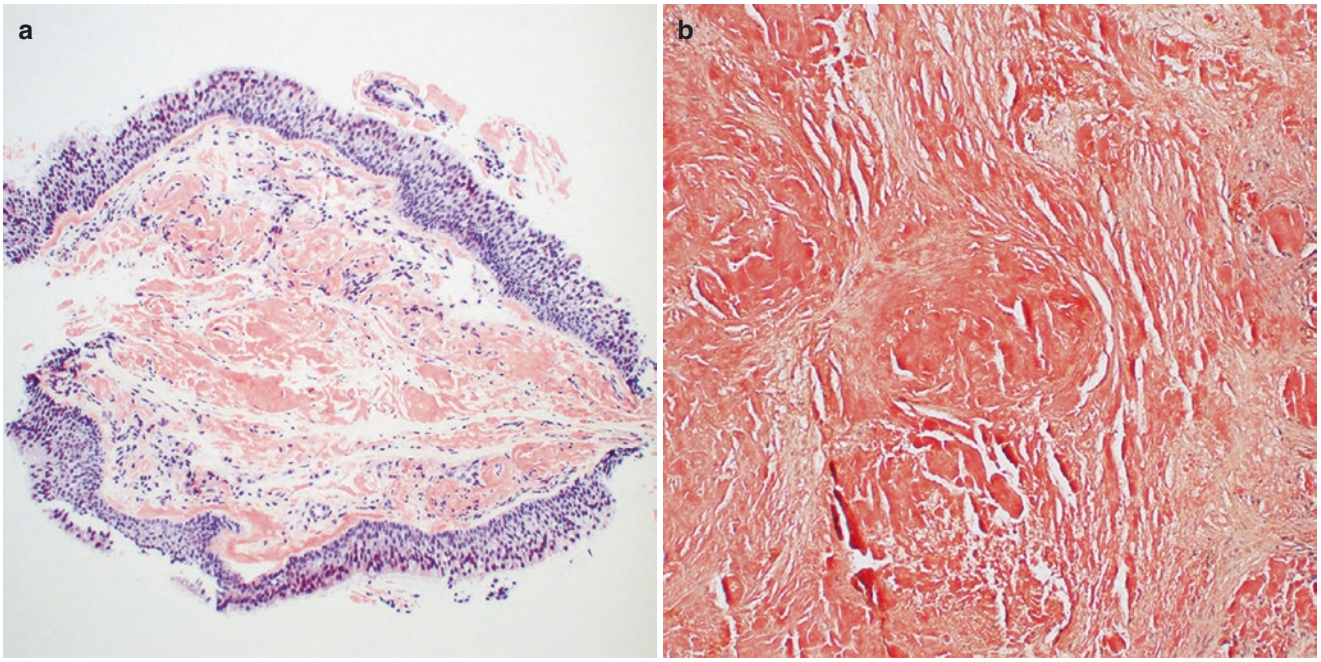

Fig. 8.31 (**a**, **b**) The amyloid deposits show bright orange-red staining with a Congo red histochemical stain

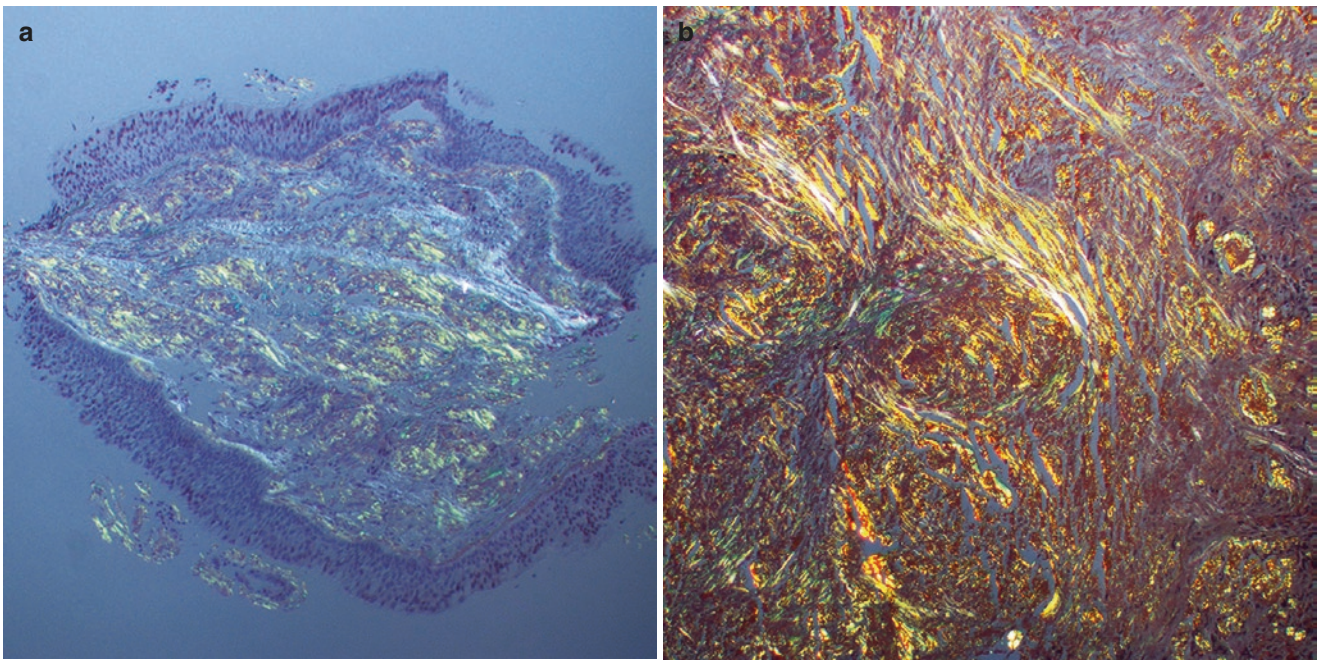

Fig. 8.32 (**a**, **b**) Under polarized light, amyloid will typically demonstrate apple green birefringence

walls in diffuse pulmonary LCDD. In this type, the deposits may also form tiny nodular lesions in the interstitium with associated lymphoplasmacytic and giant cell reaction. In the nodular form, the lung parenchyma will contain extracellular nodular aggregates of the same material. Multinucleated giant cells and collections of plasma cells or lymphocytes are often identified. Foci of calcification and ossification can be seen in both types of the condition.

8.8.3 Laboratory, Histochemical, Immunohistochemical, and Other Ancillary Investigations

Analogous to amyloidosis, serum or urine electrophoresis will often display the presence of monoclonal immunoglobulins or free light chains [145]. In contrast to amyloidosis, these light chains are more often of the κ rather than the λ type [145]

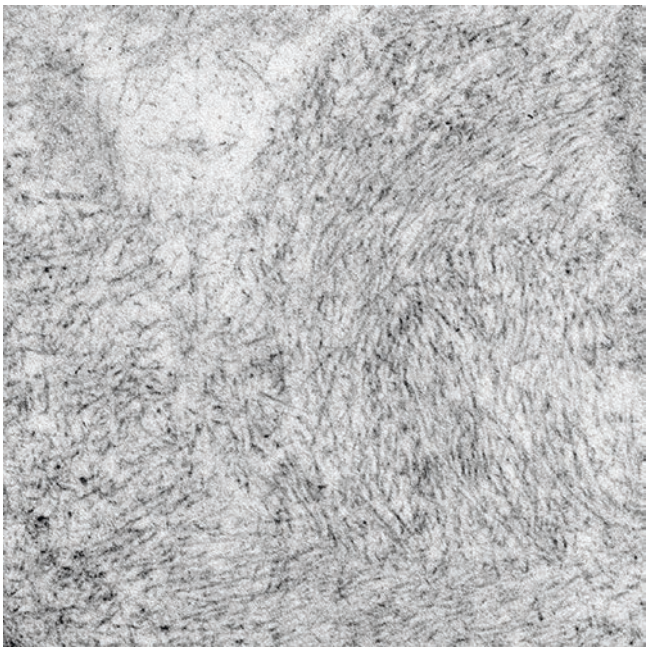

Fig. 8.33 Electron microscopy will highlight the non-branching fibrillar structure of the amyloid deposits. (Courtesy of Dr. S Dhingra, Houston, USA)

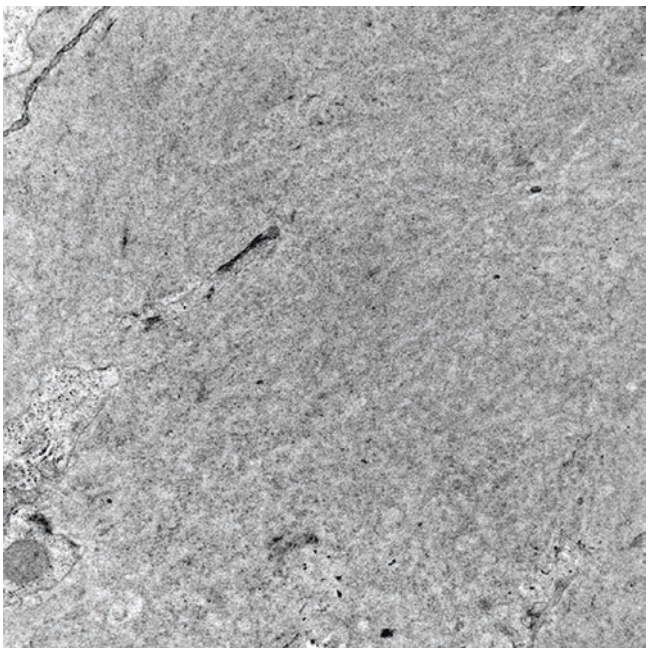

Fig. 8.34 Subtle granular deposits, as opposed to the fibrillary structures of amyloid, can be seen in this case of light chain deposition disease using electron microscopy. (Courtesy of Dr. S Dhingra, Houston, USA)

Table 8.6 Pulmonary amyloidosis versus pulmonary light chain deposition disease

	Pulmonary amyloidosis	Pulmonary light chain deposition disease
Age at presentation	7th decade	6th decade
Sex ratio	M = F	M > F
Associated diseases	Plasma cell dyscrasia MGUS Multiple myeloma Waldenström macroglobulinemia Chronic inflammatory conditions	Plasma cell dyscrasia MGUS Multiple myeloma Waldenström macroglobulinemia Lymphoplasmacytic lymphoma Chronic lymphocytic leukemia MALT lymphoma Sjögren disease
Disease patterns	Diffuse alveolar-septal Nodular Tracheobronchial	Diffuse Nodular
Light chain type	Mostly λ	Mostly κ
Histochemical stains	Congo red positive	Congo red negative
Electron microscopy	Non-branching 8–10 μm fibrils	Amorphous granular deposits
Mass spectrometry analysis	Identification of amyloid-associated peptides[a]	Absence of amyloid-associated peptides[a]

MGUS monoclonal gammopathy of uncertain significance
[a]amyloid-associated peptides: serum P component, apolipoprotein A-I, apolipoprotein A-IV, apolipoprotein E

(Table 8.6). Furthermore, non-amyloid light chains are non-reactive with Congo red and fail to display apple-green birefringence under polarized light. Electron microscopy typically reveals granular material instead of the fibrils seen in amyloidosis [145, 149, 156, 159] (Fig. 8.34). Mass spectrometry techniques can further confirm the diagnosis in difficult cases [160] (Table 8.6).

8.8.4 Differential Diagnosis

First and foremost, pulmonary LCDD must be distinguished from pulmonary amyloidosis. Both conditions show significant overlap in terms of clinical presentation, radiologic imaging, and morphological features. As mentioned above, histochemical, ultrastructural, or other ancillary techniques

are often required to separate these entities. In this context, the most important distinguishing features include (1) negative reaction with Congo red histochemical staining and absence of apple-green birefringence in cases of pulmonary LCDD compared to pulmonary amyloidosis; (2) more common presence of κ light chain immunoglobulins in LCDD as compared to amyloidosis; (3) granular appearance of deposits on ultrastructural examination in LCDD versus fibrillary deposits in amyloidosis; and (4) absence of amyloid-associated proteins on mass spectrometry proteomic analysis in pulmonary LCDD (Table 8.6). Moreover, just like in cases of amyloidosis, pulmonary LCDD must be separated from interstitial pulmonary fibrosis and pulmonary hyalinizing granuloma using similar criteria as mentioned above. Lastly, IgG4-related disease can involve the lung in the form of solitary or multiple nodules that can closely mimic nodular LCDD. The key histological features of this condition include storiform-type fibrosis, dense lymphoplasmacytic infiltrate, obliterative phlebitis, and at least 50 IgG4+ plasma cells per high power field [161]. In contrast, fibrosis and vasculitis are not typical findings in LCDD, and the number of IgG4+ plasma cells is not increased.

References

1. McChesney T. Placental transmogrification of the lung: a unique case with remarkable histopathologic features. Lab Investig. 1979;40:245–6.
2. Fidler ME, Koomen M, Sebek B, et al. Placental transmogrification of the lung, a histologic variant of giant bullous emphysema. Clinicopathological study of three further cases. Am J Surg Pathol. 1995;19:563–70.
3. Brüstle K, Lema S, Komminoth P, et al. Placental transmogrification of the lung presenting as progressive symptomatic bullous emphysema. Thorax. 2017;72:284–5.
4. Ventura L, Gnetti L, Silini EM, et al. Placental transmogrification of the lung presenting as a giant bulla associated with a pulmonary hamartoma. Ann Thorac Surg. 2016;102:e61.
5. Mark EJ, Muller KM, McChesney T, et al. Placentoid bullous lesion of the lung. Hum Pathol. 1995;26:74–9.
6. Hochholzer L, Moran CA, Koss MN. Pulmonary lipomatosis: a variant of placental transmogrification. Mod Pathol. 1997;10:846–9.
7. Moran CA, Suster S. Unusual non-neoplastic lesions of the lung. Semin Diagn Pathol. 2007;24:199–208.
8. Ma DJ, Liu HS, Li SQ, et al. Placental transmogrification of the lung: case report and systematic review of the literature. Medicine (Baltimore). 2017;96:e7733.
9. Vogel-Claussen J, Kulesza P, Macura KJ. Placental transmogrification of the lung. J Thorac Imaging. 2005;20:233–5.
10. Ortiz S, Tortosa F. Pulmonary placental transmogrification: the last 16 years in a reference centre. Rev Port Pneumol (2006). 2017;23:164–6.
11. Santana AN, Canzian M, Stelmach R, et al. Placental transmogrification of the lung presenting as giant bullae with soft-fatty components. Eur J Cardiothorac Surg. 2008;33:124–6.
12. Jenkins JM, Attia RQ, Green A, et al. A case of pulmonary placental transmogrification. Asian Cardiovasc Thorac Ann. 2016;24:811–3.
13. Xu R, Murray M, Jagirdar J, et al. Placental transmogrification of the lung is a histologic pattern frequently associated with pulmonary fibrochondromatous hamartoma. Arch Pathol Lab Med. 2002;126:562–6.
14. Cavazza A, Lantuejoul S, Sartori G, et al. Placental transmogrification of the lung: clinicopathologic, immunohistochemical and molecular study of two cases, with particular emphasis on the interstitial clear cells. Hum Pathol. 2004;35:517–21.
15. Rosen SH, Castleman B, Liebow AA. Pulmonary alveolar proteinosis. N Engl J Med. 1958;258:1123–42.
16. Gordon IO, Cipriani N, Arif Q, et al. Update in nonneoplastic lung diseases. Arch Pathol Lab Med. 2009;133:1096–105.
17. Trapnell BC, Whitsett JA, Nakata K. Pulmonary alveolar proteinosis. N Engl J Med. 2003;349:2527–39.
18. Dranoff G, Mulligan RC. Activities of granulocyte-macrophage colony-stimulating factor revealed by gene transfer and gene knockout studies. Stem Cells. 1994;12:173–82.
19. Stanley E, Lieschke GJ, Grail D, et al. Granulocyte/macrophage colony-stimulating factor-deficient mice show no major perturbation of hematopoiesis but develop a characteristic pulmonary pathology. Proc Natl Acad Sci U S A. 1994;91:5592–6.
20. Cordonnier C, Fleury-Feith J, Escudier E, et al. Secondary alveolar proteinosis is a reversible cause of respiratory failure in leukemic patients. Am J Respir Crit Care Med. 1994;149:788–94.
21. Ioachimescu OC, Kavuru MS. Pulmonary alveolar proteinosis. Chron Respir Dis. 2006;3:149–59.
22. Doerschuk CM. Pulmonary alveolar proteinosis--is host defense awry? N Engl J Med. 2007;356:547–9.
23. Khan A, Agarwal R. Pulmonary alveolar proteinosis. Respir Care. 2011;56:1016–28.
24. Rubin E, Weisbrod GL, Sanders DE. Pulmonary alveolar proteinosis: relationship to silicosis and pulmonary infection. Radiology. 1980;135:35–41.
25. Holbert JM, Costello P, Li W, et al. CT features of pulmonary alveolar proteinosis. AJR Am J Roentgenol. 2001;176:1287–94.
26. Huddleston CB, Bloch JB, Sweet SC, et al. Lung transplantation in children. Ann Surg. 2002;236:270–6.
27. Numata A, Matsuishi E, Koyanagi K, et al. Successful therapy with whole-lung lavage and autologous peripheral blood stem cell transplantation for pulmonary alveolar proteinosis complicating acute myelogenous leukemia. Am J Hematol. 2006;81:107–9.
28. Kavuru MS, Sullivan EJ, Piccin R, et al. Exogenous granulocyte-macrophage colony-stimulating factor administration for pulmonary alveolar proteinosis. Am J Respir Crit Care Med. 2000;161:1143–8.
29. Luisetti M, Rodi G, Perotti C, et al. Plasmapheresis for treatment of pulmonary alveolar proteinosis. Eur Respir J. 2009;33:1220–2.
30. Borie R, Debray MP, Laine C, et al. Rituximab therapy in autoimmune pulmonary alveolar proteinosis. Eur Respir J. 2009;33:1503–6.
31. Seymour JF, Presneill JJ. Pulmonary alveolar proteinosis: progress in the first 44 years. Am J Respir Crit Care Med. 2002;166:215–35.
32. Lin Z, deMello DE, Batanian JR, et al. Aberrant SP-B mRNA in lung tissue of patients with congenital alveolar proteinosis (CAP). Clin Genet. 2000;57:359–69.
33. Williams GD, Christodoulou J, Stack J, et al. Surfactant protein B deficiency: clinical, histological and molecular evaluation. J Paediatr Child Health. 1999;35:214–20.
34. Martin RJ, Coalson JJ, Rogers RM, et al. Pulmonary alveolar proteinosis: the diagnosis by segmental lavage. Am Rev Respir Dis. 1980;121:819–25.
35. Maygarden SJ, Iacocca MV, Funkhouser WK, et al. Pulmonary alveolar proteinosis: a spectrum of cytologic, histochemical, and

ultrastructural findings in bronchoalveolar lavage fluid. Diagn Cytopathol. 2001;24:389–95.
36. Wang BM, Stern EJ, Schmidt RA, et al. Diagnosing pulmonary alveolar proteinosis. A review and an update. Chest. 1997;111:460–6.
37. Costello JF, Moriarty DC, Branthwaite MA, et al. Diagnosis and management of alveolar proteinosis: the rôle of electron microscopy. Thorax. 1975;30:121–32.
38. Harbitz F. Extensive calcification of the lungs as a distinct disease. Arch Intern Med. 1918;21:139–46.
39. Puhr L. Mikrolithiasis alveolaris pulmonum. Virchows Arch. 1933;290:156–60.
40. Huqun, Izumi S, Miyazawa H, et al. Mutations in the SLC34A2 gene are associated with pulmonary alveolar microlithiasis. Am J Respir Crit Care Med. 2007;175:263–8.
41. Tachibana T, Hagiwara K, Johkoh T. Pulmonary alveolar microlithiasis: review and management. Curr Opin Pulm Med. 2009;15:486–90.
42. Moran CA, Hochholzer L, Hasleton PS, et al. Pulmonary alveolar microlithiasis. A clinicopathologic and chemical analysis of seven cases. Arch Pathol Lab Med. 1997;121:607–11.
43. Poelma DL, Ju MR, Bakker SC, et al. A common pathway for the uptake of surfactant lipids by alveolar cells. Am J Respir Cell Mol Biol. 2004;30:751–8.
44. Mariotta S, Ricci A, Papale M, et al. Pulmonary alveolar microlithiasis: report on 576 cases published in the literature. Sarcoidosis Vasc Diffuse Lung Dis. 2004;21:173–81.
45. Castellana G, Lamorgese V. Pulmonary alveolar microlithiasis. World cases and review of the literature. Respiration. 2003;70:549–55.
46. Fuleihan FJ, Abboud RT, Balikian JP, et al. Pulmonary alveolar microlithiasis: lung function in five cases. Thorax. 1969;24:84–90.
47. Jönsson ÅL, Simonsen U, Hilberg O, et al. Pulmonary alveolar microlithiasis: two case reports and review of the literature. Eur Respir Rev. 2012;21:249–56.
48. Coetzee T. Pulmonary alveolar microlithiasis with involvement of the sympathetic nervous system and gonads. Thorax. 1970;25:637–42.
49. Richardson J, Slovis B, Miller G, et al. Development of pulmonary alveolar microlithiasis in a renal transplant recipient. Transplantation. 1995;59:1056–7.
50. Ferreira Francisco FA, Pereira e Silva JL, Hochhegger B, et al. Pulmonary alveolar microlithiasis. State-of-the-art review. Respir Med. 2013;107:1–9.
51. Korn MA, Schurawitzki H, Klepetko W, et al. Pulmonary alveolar microlithiasis: findings on high-resolution CT. AJR Am J Roentgenol. 1992;158:981–2.
52. Cluzel P, Grenier P, Bernadac P, et al. Pulmonary alveolar microlithiasis: CT findings. J Comput Assist Tomogr. 1991;15:938–42.
53. Marchiori E, Gonçalves CM, Escuissato DL, et al. Pulmonary alveolar microlithiasis: high-resolution computed tomography findings in 10 patients. J Bras Pneumol. 2007;33:552–7.
54. Gasparetto EL, Tazoniero P, Escuissato DL, et al. Pulmonary alveolar microlithiasis presenting with crazy-paving pattern on high resolution CT. Br J Radiol. 2004;77:974–6.
55. Stamatis G, Zerkowski HR, Doetsch N, et al. Sequential bilateral lung transplantation for pulmonary alveolar microlithiasis. Ann Thorac Surg. 1993;56:972–5.
56. Lauta VM. Pulmonary alveolar microlithiasis: an overview of clinical and pathological features together with possible therapies. Respir Med. 2003;97:1081–5.
57. Barnard NJ, Crocker PR, Blainey AD, et al. Pulmonary alveolar microlithiasis. A new analytical approach. Histopathology. 1987;11:639–45.
58. Takahashi H, Chiba H, Shiratori M, et al. Elevated serum surfactant protein A and D in pulmonary alveolar microlithiasis. Respirology. 2006;11:330–3.
59. Luschka H. Verästigte Knochenbildung im Parenchym der Lungen. Virchows Arch. 1856;10:500–5.
60. Popelka CG, Kleinerman J. Diffuse pulmonary ossification. Arch Intern Med. 1977;137:523–5.
61. Joines RW, Roggli VL. Dendriform pulmonary ossification. Report of two cases with unique findings. Am J Clin Pathol. 1989;91:398–402.
62. Kanne JP, Godwin JD, Takasugi JE, et al. Diffuse pulmonary ossification. J Thorac Imaging. 2004;19:98–102.
63. Lara JF, Catroppo JF, Kim DU, et al. Dendriform pulmonary ossification, a form of diffuse pulmonary ossification: report of a 26-year autopsy experience. Arch Pathol Lab Med. 2005;129:348–53.
64. Galloway RW, Epstein EJ, Coulshed N. Pulmonary ossific nodules in mitral value disease. Br Heart J. 1961;23:297–307.
65. Felson B, Schwarz J, Lukin RR, et al. Idiopathic pulmonary ossification. Radiology. 1984;153:303–10.
66. Ndimbie OK, Williams CR, Lee MW. Dendriform pulmonary ossification. Arch Pathol Lab Med. 1987;111:1062–4.
67. Egashira R, Jacob J, Kokosi MA, et al. Diffuse pulmonary ossification in fibrosing interstitial lung diseases: prevalence and associations. Radiology. 2017;284:255–63.
68. Chan ED, Morales DV, Welsh CH, et al. Calcium deposition with or without bone formation in the lung. Am J Respir Crit Care Med. 2002;165:1654–69.
69. Jacobs AN, Neitzschman HR, Nice CM Jr. Metaplastic bone formation in the lung. Am J Roentgenol Radium Therapy, Nucl Med. 1973;118:344–6.
70. Felson B. Thoracic calcifications. Dis Chest. 1969;56:330–43.
71. Ahari JE. Dendriform pulmonary ossification: a clinical diagnosis with a 14 year follow-up. Chest. 2007;132:701S.
72. Peros-Golubicić T, Tekavec-Trkanjec J. Diffuse pulmonary ossification: an unusual interstitial lung disease. Curr Opin Pulm Med. 2008;14:488–92.
73. Bisceglia M, Chiaramonte A, Panniello G, et al. Selected case from the Arkadi M. Rywlin international pathology slide series: diffuse dendriform pulmonary ossification: report of 2 cases with review of the literature. Adv Anat Pathol. 2015;22:59–68.
74. Woolley K, Stark P. Pulmonary parenchymal manifestations of mitral valve disease. Radiographics. 1999;19:965–72.
75. Bendayan D, Barziv Y, Kramer MR. Pulmonary calcifications: a review. Respir Med. 2000;94:190–3.
76. Kuhlman JE, Ren H, Hutchins GM, et al. Fulminant pulmonary calcification complicating renal transplantation: CT demonstration. Radiology. 1989;173:459–60.
77. Ringe JD. Hypercalcemia: symptom and syndrome. Internist (Berl). 1985;26:405–10.
78. Seifert G. Heterotopic (extraosseous) calcification (calcinosis). Etiology, pathogenesis and clinical importance. Pathologe. 1997;18:430–8.
79. Lallemand D, Lacombe P, Garel L. Metastatic pulmonary calcifications in children. Three cases. Ann Radiol (Paris). 1982;25:106–12.
80. Northcutt AD, Tio FO, Chamblin SA Jr, et al. Massive metastatic pulmonary calcification in an infant with aleukemic monocytic leukemia. Pediatr Pathol. 1985;4:219–29.
81. Cohen MC, Drut R. Metastatic pulmonary calcification with ossification in a child with acute lymphoblastic leukemia. Pediatr Pulmonol. 1999;27:134–7.
82. De Nardi P, Gini P, Molteni B, et al. Metastatic pulmonary and rectal calcifications secondary to primary hyperparathyroidism. Eur J Surg. 1996;162:735–8.

83. Nakamura M, Ohishi A, Watanabe R, et al. Adult T-cell leukemia with hypercalcemia-induced metastatic calcification in the lungs due to production of parathyroid hormone-related protein. Intern Med. 2001;40:409–13.
84. Kaburagi T, Nagai H, Sasaki T, et al. Case report of multiple myeloma associated with diffuse pulmonary calcinosis. Nihon Kyobu Shikkan Gakkai Zasshi. 1991;29:1479–83.
85. Nambu Y, Iwata T, Oida K, et al. Clinicopathological features of metastatic pulmonary calcinosis with malignant neoplasm. Nihon Kyobu Shikkan Gakkai Zasshi. 1991;29:963–70.
86. Sasaki I, Morimoto K, Koya Y, et al. An autopsy case of adult T-cell leukemia complicated with metastatic calcification of the lung. Nihon Kyobu Shikkan Gakkai Zasshi. 1991;29:105–10.
87. Sanders C, Frank MS, Rostand SG, et al. Metastatic calcification of the heart and lungs in end-stage renal disease: detection and quantification by dual-energy digital chest radiography. AJR Am J Roentgenol. 1987;149:881–7.
88. Katz S, Stanton J, McCormick G. Miliary calcification of the lungs after treated miliary tuberculosis. N Engl J Med. 1955;253:135–7.
89. Sargent EN, Balchum E, Freed AL, et al. Multiple pulmonary calcifications due to coccidioidomycosis. Am J Roentgenol Radium Therapy, Nucl Med. 1970;109:500–4.
90. Lace PA. An investigation into the aetiological factors concerned in disseminated calcification of the lungs. Med J Aust. 1968;2:951–3.
91. Kaltreider HB, Baum GL, Bogaty G, et al. So-called "metastatic" calcification of the lung. Am J Med. 1969;46:188–96.
92. Conger JD, Hammond WS, Alfrey AC, et al. Pulmonary calcification in chronic dialysis patients. Clinical and pathologic studies. Ann Intern Med. 1975;83:330–6.
93. Kuzela DC, Huffer WE, Conger JD, et al. Soft tissue calcification in chronic dialysis patients. Am J Pathol. 1977;86:403–24.
94. Ullmer E, Borer H, Sandoz P, et al. Diffuse pulmonary nodular infiltrates in a renal transplant recipient. Metastatic pulmonary calcification. Chest. 2001;120:1394–8.
95. Hartman TE, Müller NL, Primack SL, et al. Metastatic pulmonary calcification in patients with hypercalcemia: findings on chest radiographs and CT scans. AJR Am J Roentgenol. 1994;162:799–802.
96. Marchiori E, Müller NL, Souza AS Jr, et al. Unusual manifestations of metastatic pulmonary calcification: high-resolution CT and pathological findings. J Thorac Imaging. 2005;20:66–70.
97. Greenberg S, Suster B. Metastatic pulmonary calcification: appearance on high resolution CT. J Comput Assist Tomogr. 1994;18:497–9.
98. Mani TM, Lallemand D, Corone S, et al. Metastatic pulmonary calcifications after cardiac surgery in children. Radiology. 1990;174:463–7.
99. Winter EM, Pollard AJ, Chapman S, et al. Case report: pulmonary calcification after liver transplantation in children. Br J Radiol. 1995;68:923–5.
100. Johkoh T, Ikezoe J, Nagareda T, et al. Metastatic pulmonary calcification: early detection by high-resolution CT. J Comput Assist Tomogr. 1993;17:471–3.
101. McLachlan MS, Wallace M, Seneviratne C. Pulmonary calcification in renal failure. Report of three cases. Br J Radiol. 1968;41:99–106.
102. Davidson RC, Pendros JP. Calcium related cardio-respiratory death in chronic hemodialysis. Trans Am Soc Artif Intern Organs. 1967;13:36–40.
103. Engleman P, Liebow AA, Gmelich J, et al. Pulmonary hyalinizing granuloma. Am Rev Respir Dis. 1977;115:997–1008.
104. Lhote R, Haroche J, Duron L, et al. Pulmonary hyalinizing granuloma: a multicenter study of 5 new cases and review of the 135 cases of the literature. Immunol Res. 2017;65:375–85.
105. Chapman EM, Gown A, Mazziotta R, et al. Pulmonary hyalinizing granuloma with associated elevation in serum and tissue IgG4 occurring in a patient with a history of sarcoidosis. Am J Surg Pathol. 2012;36:774–8.
106. Yousem SA, Hochholzer L. Pulmonary hyalinizing granuloma. Am J Clin Pathol. 1987;87:1–6.
107. Ussavarungsi K, Khoor A, Jolles HI, et al. A 40-year-old woman with multiple pulmonary nodules. Pulmonary hyalinizing granuloma. Chest. 2014;146:e198–203.
108. Shibata Y, Kobayashi T, Hattori Y, et al. High-resolution CT findings in pulmonary hyalinizing granuloma. J Thorac Imaging. 2007;22:374–7.
109. Lien CT, Yang CJ, Yang SF, et al. Pulmonary hyalinizing granuloma mimicking multiple lung metastases: report of fluorodeoxyglucose positron emission findings. J Thorac Imaging. 2010;25:W36–9.
110. Guccion JG, Rohatgi PK, Saini N. Pulmonary hyalinizing granuloma. Electron microscopic and immunologic studies. Chest. 1984;85(4):571–3.
111. Sipe JD, Benson MD, Buxbaum JN, et al. Nomenclature 2014: amyloid fibril proteins and clinical classification of the amyloidosis. Amyloid. 2014;21:221–4.
112. Virchow R. Über eine im Gehirn und Rückenmark des Menschen aufgefundene Substanz mit der chemischen Reaktion der Cellulose. Virchows Arch. 1854;6:135–8.
113. Sipe JD, Benson MD, Buxbaum JN, et al. Amyloid fibril proteins and amyloidosis: chemical identification and clinical classification International Society of Amyloidosis 2016 nomenclature guidelines. Amyloid. 2016;23:209–2113.
114. Utz JP, Swensen SJ, Gertz MA. Pulmonary amyloidosis. The Mayo Clinic experience from 1980 to 1993. Ann Intern Med. 1996;124:407–13.
115. Cordier JF. Pulmonary amyloidosis in hematological disorders. Semin Respir Crit Care Med. 2005;26:502–13.
116. Authier FJ, Lechapt-Zalcman E, Mussini JM, et al. Marked systemic amyloid angiopathy in patients with val 107 transthyretin mutation. J Clin Neuromuscul Dis. 1999;1:82–5.
117. Ueda M, Ando Y, Haraoka K, et al. Aging and transthyretin-related amyloidosis: pathologic examinations in pulmonary amyloidosis. Amyloid. 2006;13:24–30.
118. Grogg KL, Aubry MC, Vrana JA, et al. Nodular pulmonary amyloidosis is characterized by localized immunoglobulin deposition and is frequently associated with an indolent B-cell lymphoproliferative disorder. Am J Surg Pathol. 2013;37:406–12.
119. Ikeda S, Takabayashi Y, Maejima Y, et al. Nodular lung disease with five year survival and unilateral pleural effusion in AL amyloidosis. Amyloid. 1999;6:292–6.
120. Kaplan B, Martin BM, Boykov O, et al. Co-deposition of amyloidogenic immunoglobulin light and heavy chains in localized pulmonary amyloidosis. Virchows Arch. 2005;447:756–61.
121. Beer TW, Edwards CW. Pulmonary nodules due to reactive systemic amyloidosis (AA) in Crohn's disease. Thorax. 1993;48:1287–8.
122. Roden AC, Aubry MC, Zhang K, et al. Nodular senile pulmonary amyloidosis: a unique case confirmed by immunohistochemistry, mass spectrometry, and genetic study. Hum Pathol. 2010;41:1040–5.
123. Yang MC, Blutreich A, Das K. Nodular pulmonary amyloidosis with an unusual protein composition diagnosed by fine-needle aspiration biopsy: a case report. Diagn Cytopathol. 2009;37:286–9.
124. Dacic S, Colby TV, Yousem SA. Nodular amyloidoma and primary pulmonary lymphoma with amyloid production: a differential diagnostic problem. Mod Pathol. 2000;13:934–40.
125. Hui AN, Koss MN, Hochholzer L, et al. Amyloidosis presenting in the lower respiratory tract. Clinicopathologic, radiologic, immu-

nohistochemical, and histochemical studies on 48 cases. Arch Pathol Lab Med. 1986;110:212–8.
126. da Costa P, Corrin B. Amyloidosis localized to the lower respiratory tract: probable immunoamyloid nature of the tracheobronchial and nodular pulmonary forms. Histopathology. 1985;9:703–10.
127. O'Regan A, Fenlon HM, Beamis JF Jr, et al. Tracheobronchial amyloidosis. The Boston University experience from 1984 to 1999. Medicine (Baltimore). 2000;79:69–79.
128. Capizzi SA, Betancourt E, Prakash UB. Tracheobronchial amyloidosis. Mayo Clin Proc. 2000;75:1148–52.
129. Celli BR, Rubinow A, Cohen AS, et al. Patterns of pulmonary involvement in systemic amyloidosis. Chest. 1978;74:543–7.
130. Kirbaş G, Dağli CE, Tanrikulu AC, et al. Unusual combination of tracheobronchopathia osteochondroplastica and AA amyloidosis. Yonsei Med J. 2009;50:721–4.
131. Kyle RA, Greipp PR. Amyloidosis (AL). Clinical and laboratory features in 229 cases. Mayo Clin Proc. 1983;58:665–83.
132. Wechalekar AD, Gillmore JD, Bird J, et al. BCSH Committee. Guidelines on the management of AL amyloidosis. Br J Haematol. 2015;168:186–206.
133. Livneh A, Zemer D, Langevitz P, et al. Colchicine in the treatment of AA and AL amyloidosis. Semin Arthritis Rheum. 1993;23:206–14.
134. Gertz MA, Benson MD, Dyck PJ, et al. Diagnosis, prognosis, and therapy of transthyretin amyloidosis. J Am Coll Cardiol. 2015;66:2451–66.
135. Ussavarungsi K, Yi ES, Maleszewski JJ, et al. Clinical relevance of pulmonary amyloidosis: an analysis of 76 autopsy-derived cases. Eur Respir J. 2017;49(2). pii: 1602313.
136. Chen KT. Amyloidosis presenting in the respiratory tract. Pathol Annu. 1989;24:253–73.
137. Rubinow A, Celli BR, Cohen AS, et al. Localized amyloidosis of the lower respiratory tract. Am Rev Respir Dis. 1978;118:603–11.
138. Condon RE, Pinkham RD, Hames GH. Primary isolated nodular pulmonary amyloidosis. Report of a case. J Thorac Cardiovasc Surg. 1964;48:498–505.
139. Weiss L. Isolated multiple nodular pulmonary amyloidosis. Am J Clin Pathol. 1960;33:318–29.
140. Khoor A, Colby TV. Amyloidosis of the lung. Arch Pathol Lab Med. 2017;141:247–54.
141. Lewis JE, Olsen KD, Kurtin PJ, et al. Laryngeal amyloidosis: a clinicopathologic and immunohistochemical review. Otolaryngol Head Neck Surg. 1992;106:372–7.
142. Pickford HA, Swensen SJ, Utz JP. Thoracic cross-sectional imaging of amyloidosis. AJR Am J Roentgenol. 1997;168:351–5.
143. Kirchner J, Jacobi V, Kardos P, et al. CT findings in extensive tracheobronchial amyloidosis. Eur Radiol. 1998;8:352–4.
144. Neben-Wittich MA, Foote RL, Kalra S. External beam radiation therapy for tracheobronchial amyloidosis. Chest. 2007;132:262–7.
145. Bhargava P, Rushin JM, Rusnock EJ, et al. Pulmonary light chain deposition disease: report of five cases and review of the literature. Am J Surg Pathol. 2007;31:267–76.
146. Laden SA, Cohen ML, Harley RA. Nodular pulmonary amyloidosis with extrapulmonary involvement. Hum Pathol. 1984;15:594–7.
147. Sipe JD. Serum amyloid A: from fibril to function. Current status. Amyloid. 2000;7:10–2.
148. Vrana JA, Gamez JD, Madden BJ, et al. Classification of amyloidosis by laser microdissection and mass spectrometry-based proteomic analysis in clinical biopsy specimens. Blood. 2009;114:4957–9.
149. Kijner CH, Yousem SA. Systemic light chain deposition disease presenting as multiple pulmonary nodules. A case report and review of the literature. Am J Surg Pathol. 1988;12:405–13.
150. Rostagno A, Frizzera G, Ylagan L, et al. Tumoral non-amyloidotic monoclonal immunoglobulin light chain deposits ('aggregoma'): presenting feature of B-cell dyscrasia in three cases with immunohistochemical and biochemical analyses. Br J Haematol. 2002;119:62–9.
151. Khoor A, Myers JL, Tazelaar HD, et al. Amyloid-like pulmonary nodules, including localized light-chain deposition: clinicopathologic analysis of three cases. Am J Clin Pathol. 2004;121:200–4.
152. Morinaga S, Watanabe H, Gemma A, et al. Plasmacytoma of the lung associated with nodular deposits of immunoglobulin. Am J Surg Pathol. 1987;11:989–95.
153. Piard F, Yaziji N, Jarry O, et al. Solitary plasmacytoma of the lung with light chain extracellular deposits: a case report and review of the literature. Histopathology. 1998;32:356–61.
154. Stokes MB, Jagirdar J, Burchstin O, et al. Nodular pulmonary immunoglobulin light chain deposits with coexistent amyloid and nonamyloid features in an HIV-infected patient. Mod Pathol. 1997;10:1059–65.
155. Colombat M, Stern M, Groussard O, et al. Pulmonary cystic disorder related to light chain deposition disease. Am J Respir Crit Care Med. 2006;173:777–80.
156. Sheard S, Nicholson AG, Edmunds L, et al. Pulmonary light-chain deposition disease: CT and pathology findings in nine patients. Clin Radiol. 2015;70:515–22.
157. Rho L, Qiu L, Strauchen JA, et al. Pulmonary manifestations of light chain deposition disease. Respirology. 2009;14:767–70.
158. Arrossi AV, Merzianu M, Farver C, et al. Nodular pulmonary light chain deposition disease: an entity associated with Sjögren syndrome or marginal zone lymphoma. J Clin Pathol. 2016;69:490–6.
159. Khoor A, Colby TV. Amyloidosis of the lung. Arch Pathol Lab Med. 2017;141:247–54.
160. Colombat M, Holifanjaniaina S, Guillonneau F, et al. Mass spectrometry-based proteomic analysis: a good diagnostic tool for cystic lung light chain deposition disease. Am J Respir Crit Care Med. 2013;188:404–5.
161. Cheuk W, Chan JK. IgG4-related sclerosing disease: a critical appraisal of an evolving clinicopathologic entity. Adv Anat Pathol. 2010;17:303–32.